



Amston Lake

2020 Water Quality Monitoring

Prepared for the
Amston Lake Tax District
Hebron & Lebanon, CT
February 13, 2021

This page was intentionally left blank.

EXECUTIVE SUMMARY

Aquatic Ecosystem Research (AER) was engaged by the Amston Lake Tax District to assess water quality monitoring data collected from a deep-water site on Amston Lake and from 13 stormwater collection sites along the perimeter of the lake. A summary of important findings is provided below.

- The lake was stratified from May 20th through August 26th.
 - Anoxic conditions were observed at approximately 7m of depth starting on July 2nd, at 6 and 7m of depth between July 13th and August 26th, and at 7m of depth on September 9th.
- Epilimnetic total phosphorus concentrations were, on average, low (11.4µg/L) and characteristic of early mesotrophic conditions.
 - The highest epilimnetic concentration (23µg/L) occurred on May 7th, before stratification, implicating a watershed-based (allochthonous) source.
- Hypolimnetic total phosphorus concentrations were higher, averaging 30.6µg/L.
 - Hypolimnetic concentrations were not notably different from epilimnetic or metalimnetic concentrations until July 29th through August 26th which followed a protracted period of anoxic conditions above the lake sediments.
 - Hypolimnetic concentrations substantially decreased following the loss of stratification and mixing of the water column.
 - This scenario characterizes an internal (autochthonous) source of nutrients but did not appear to greatly impact epilimnetic concentrations.
- Epilimnetic total Kjeldahl nitrogen levels averaged 499µg/L with the lowest concentration (380µg/L) occurring on May 7th.
 - The nitrogen levels were characteristic of mesotrophic productivity; however, algal productivity appears limited by phosphorus based on the Redfield ratio.
- Hypolimnetic and metalimnetic total Kjeldahl nitrogen averaged 689 and 458µg/L, respectively.
 - Hypolimnetic levels, and to a lesser extent, metalimnetic levels increased between May 7th and August 26th with hypolimnetic concentrations on the latter date reaching 1,300µg/L; approximately half of that was in the form of ammonia.
 - This also supports autochthonous nutrient sources due to anoxic conditions at the sediment-water interface.

- Measurable amounts of ammonia were observed in most of the water samples, regardless of depth.
- Average Secchi disk transparency (5.38m) and chlorophyll-a concentration (3.96µg/L) were also characteristic of early mesotrophic productivity.
 - Secchi disk transparency was greatest at the beginning and end of the season but was likely underestimated since it was limited by the maximum depth at the sampling site (approximately 7m).
 - Season lows of approximately 4m occurred between July 13th and August 26th.
 - Season low chlorophyll-a concentrations (<1.4µg/L), were measured at the beginning and end of the season; highest concentrations were found in samples collected on July 2nd (7.7µg/L) and July 29th (10.2µg/L).
 - The inverse relationship between Secchi transparency and chlorophyll-a is to be expected.
- There was a wide range of specific conductance measurements in 2020.
 - Epilimnetic levels were between 112 to 131µS/cm from May 7th to September 24th.
 - The October 20th level was 163µS/cm.
 - Hypolimnetic levels gradually increased from 117 to 153µS/cm from May 7th through August 26th while the lake was stratified.
 - On September 24th, after the water column mixed, hypolimnetic specific conductance was 94µS/cm, which was notably lower than the corresponding epilimnetic level.
 - The October 20th hypolimnetic level was also 163µS/cm.
 - The October 20, 2020 levels at both strata were the highest recorded over the last two years
 - Changes in ion concentrations were not commensurate with change in specific conductance at the end of 2020.
 - Total dissolved solids exhibited the same pattern as specific conductance.
- On a milliequivalent basis, sodium and chloride were similar in concentration and the dominant ions measured in the epilimnetic samples.
 - Calcium and alkalinity were also similar to each other in concentration but were lower than levels of sodium and chloride.
 - Sodium chloride concentrations may be related to use of deicing salts in the winter.
- Results from algae analyses supported the early mesotrophic characterization of the lake.

- Cell concentrations were generally low, reaching a maximum concentration of 6,236 cell/mL on July 29th.
 - Cyanobacteria (aka Blue-green algae) became dominant by July 29th.
 - On a biovolume basis, the only time Cyanobacteria dominated the algal community was on October 20th.
- Results from analyses for *Escherichia coli* (*E. coli*) in eight samples collected at beaches and the shoreline along the North Cove were assessed.
 - Results of samples collected on November 20, 2019 ranged from <10 to 52 organisms per 100mL with the highest concentrations from samples collected in North Cove.
 - Results from samples collected on July 20, 2020 were all ≤ 10 organisms per 100mL
 - All results were below the State threshold of 235 organisms per 100mL and indicative of good sanitary water quality conditions.
- Stormwater samples were collected from 13 sites around the lake on April 9th and May 1st.
 - Average phosphorus and nitrogen levels were significantly higher in the April 9th samples.
 - By May 1st, stormwater total phosphorus and total Kjeldahl nitrogen levels were comparable to the May 7th levels in the lake.
 - Mitigating nutrients in the “first flush” in the spring will be determined by land use practices in specific drainage basins.
 - Analyses of ionic constituents in the stormwater samples revealed that sodium and chloride were the dominant ions on a meq/L basis.
 - Those two were closely related and both exhibited a strong relationship with stormwater specific conductance.
 - Deicing road salts may be contributing to the dissolved salt levels in the lake.
- Statistical analyses with Multiple Linear Regression (MLR) and Analyses of Variance (ANOVA) were applied to the Amston Lake data since 1994, and the stormwater data since 2001.
 - Analyses were applied to the entire datasets and subsets of each, e.g., lake epilimnetic and hypolimnetic subsets, and Hebron and Lebanon stormwater datasets.
 - Significant changes ($p < 0.05$) were observed in both the lake and stormwater datasets.
 - Significant changes in the lake over time included increases in nutrients and specific conductance.

- Significant changes in stormwater included reductions of nutrients and specific conductance levels over time.
 - Hypothesis as to why the opposite trends in the lake and stormwater are provided.
- Recommendations are provided and included:
 - Continuation of the lake and stormwater monitoring program.
 - Attempt to sample just after the first major spring thaw or rain event.
 - Developing strategies for cross-checking data, e.g., specific conductance.
 - Randomly sample in duplicate that are analyzed by the Lake Health Committee of the Amston Lake Tax District and send one half to Phoenix Environmental



Amston Lake 2020 Water Quality Monitoring

TABLE OF CONTENTS

Executive Summary.....	3
Introduction	9
Methods.....	9
Temperature and Oxygen Profiles.....	13
Nutrients	15
Total Phosphorus.....	15
Nitrogen	17
TN:TP Ratio.....	18
Secchi Transparency and Chlorophyll- <i>a</i>	19
Secchi Disk Transparency.....	20
Chlorophyll- <i>a</i> Concentrations	20
Alkalinity and pH.....	20
Specific Conductance and Total Dissolved Solids.....	22
Cation and Anion Concentrations.....	23
Algal Dynamics.....	25
Public Health Monitoring	28
2020 Lake Water Quality Assessment.....	29
Trophic Status	29
Ionic Concentrations	30
Stormwater.....	32
Nutrients.....	32
Ion concentrations	33
Stormwater Assessment.....	36
Water Quality Trends.....	37
Lake Trends.....	37
Stormwater.....	38
Recommendations.....	41

References.....42
Appendix A. Algal Community Data.....44
Appendix B. Base Cations, Chloride, and Alkalinity54
Appendix C. Statistical Analyses56

INTRODUCTION

Amston Lake (41°37'32.86"N, 72°19'42.425"W) is an approximately 188-acre lake located in the municipalities of Hebron and Lebanon, CT. This natural lake has a maximum depth of 7.9 meters, a mean depth of 2.7 meters and contains approximately 2.1×10^6 cubic meters of water (AER 2019).

The lake's relatively small watershed is approximately 680 acres or just over one square mile (ECRCDA 1985) yielding a small watershed to lake ratio of 3.6. The lake and watershed are situated in the Eastern Uplands geological region of Connecticut; bedrock types of this region are crystalline in nature and largely comprised of erosion resistant schists, gneiss, and some granites and pegmatites (Bell 1985, ECRCDA 1985).

The lake is fed by wetlands and three small streams; surface waters enter the lake primarily from the south. The lake level is regulated by a small dam where waters drain into a tributary that connects with Raymond Brook. Raymond Brook flows into the Jeremy River, which flows to the Salmon River. Amston Lake is located in the Raymond Brook subregion of the Salmon River watershed.

The lake is private and managed by the Amston Lake Tax District (ALTD). The ALTD committee which oversees the volunteer lake water quality monitoring and stormwater quality monitoring programs is the Lake Health Committee. Data that dates back to 1994 have been compiled for the lake by the Committee; data from stormwater sites dates back to 2001.

The ALTD engaged AER to provide several services in 2020. The first was a quantitative aquatic plant survey which was performed on July 18th and reported on in December of 2020. The second service was assessments of lake water quality and stormwater quality data collected by the Lake Health Committee in 2020. This report details those water quality assessments based on data provided to AER.

METHODS

All field data and water sample collections from Amston Lake were performed at a site of maximum depth (Fig. 1) by Jeff and Fran Arpin. Data collected at the site included water temperature and dissolved oxygen concentrations measured at 0.5 meters (m) from the surface and at one-meter interval throughout the water column. Water clarity or transparency was measured using a standard Secchi disk. Water samples were collected on the following dates for laboratory analyses: May 7th, June 2nd, July 2nd, July 29th, August 26th, September 24th, and October 20th. Samples were collected at 1m of depth from the surface, and at approximately 0.5m from the bottom on each occasion; additionally, a mid-depth sample was collected on May 7th before the lake stratified

and monthly from June 2nd to August 26th while the water column was stratified. Additional site visits occurred on May 20th, June 17th, July 13th, August 12th, September 9th, and October 6th for field data collections but did not include water sample collections.

Many of the analyses of water samples were performed by Phoenix Environmental Laboratories, Inc. in Manchester, CT. Other analyses were performed by Jeff Arpin. A list of analytes, who performed them, and on which samples is provided in Table 1.

Analyses of algae samples were performed by AER. Whole water samples for analyses of algae cell concentrations were preserved with Lugol's solution, then treated with hydrostatic pressure to collapse gas vesicles of the cyanobacteria cells (Lawton et al. 1999). Known volumes of the preserved samples were concentrated into smaller volumes with centrifugation and a vacuum pump / filtration flask system. Portions of those concentrates were pipetted into a counting chamber, then genus-level algal cell enumerations were performed by counting cells in a subset of the chamber's fields using an inverted Nikon Diaphot research microscope. Those counts were then corrected to be reflective of the whole water samples. Concentrated samples collected in the field with a 10µm mesh plankton were also examined with microscopy to establish a qualitative list of genera.

Thermal resistance to mixing (RTRM), which is an assessment of the ability of two different water volumes – that differ in temperature and density – to mix, was calculated using the Relative Thermal Resistance to Mixing (RTRM) formula: $(D_1 - D_2)/(D' - D^0)$, where D_1 is the density of upper water volume, D_2 is the density of the lower water volume, D' is the density of water at 5°C, and D^0 is the density of water at 4°C. RTRM values ≥ 80 indicate strong resistance to mixing, which means that those layers are not mixing.

Stormwater samples were collected by the volunteer of the Lake Health Committee at 13 sites along the perimeter of the lake (Fig. 1) on April 9th and May 1st of 2020.

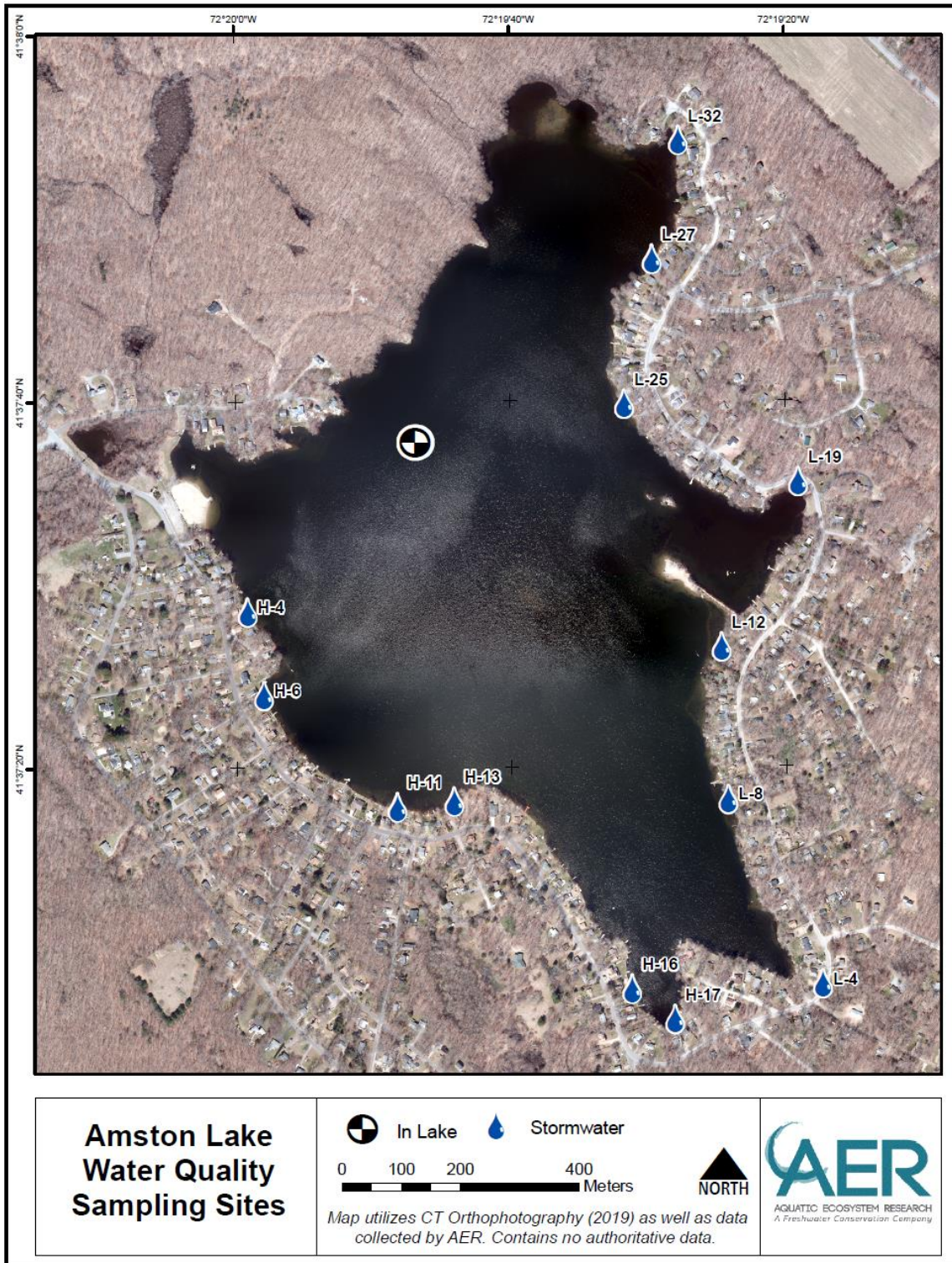


Figure 1. Map of Amston Lake identifying locations of lake water quality sampling and storm-water quality sampling sites.

Table 1. List of dates, sites, and analyses performed at Amston Lake and 13 stormwater sites in 2020.

2020 Dates	Sites	Phoenix List	Arpin List	AER List	Field Data
April 9 th	Stormwater	✓	✓		
May 1 st	Stormwater	✓	✓		
May 7 th	Lake	✓	✓	✓	✓
May 20 th	Lake				✓
June 2 nd	Lake	✓	✓	✓	✓
June 17 th	Lake				✓
July 2 nd	Lake	✓	✓	✓	✓
July 13 th	Lake				✓
July 29 th	Lake	✓	✓	✓	✓
August 12 th	Lake				✓
August 26 th	Lake	✓	✓	✓	✓
September 9 th	Lake				✓
September 24 th	Lake	✓	✓	✓	✓
October 6 th	Lake				✓
October 20 th	Lake	✓	✓	✓	✓
Phoenix List	Total Phosphorus, Total Kjeldahl Nitrogen, Ammonia, Nitrate, Nitrite, Alkalinity, Chloride, Sodium, Potassium, Calcium, Magnesium, Turbidity, and Chlorophyll-a*				
Arpin List	Specific Conductance, Salinity, Total Dissolved Solids, Resistivity, pH				
AER List	Quantitative and Qualitative Analyses of Algae Samples				
Field Data	Temperature, Dissolved Oxygen, Secchi Transparency**				

* Chlorophyll-*a* was only analyzed in samples from 1m of depth from the lake

** Secchi disk transparency was only measured at the deep-water site in the lake.

TEMPERATURE AND OXYGEN PROFILES

Temperature profile data allow for the assessment of thermal characteristics of the water column by providing the means to calculate where layers of water were and were not mixing as a result of temperature/density differences. In shallow New England lakes stratification can occur but it may be short in duration as energy from wind can mix the water column. In deeper lakes, a middle transitional layer (aka metalimnion) separates the upper warmer layer (aka epilimnion) from lower, colder waters below (aka hypolimnion). Within the metalimnion resides the thermocline, which is the layer between strata where temperature/density changes are greatest with increasing depth. These conditions will often persist in deeper lakes for the entire summer and early fall until weak thermal separation affords bottom to top mixing.

An understanding of oxygen concentrations is important for several reasons. An oxygen concentration of 5mg/L is generally thought to be the threshold limit of sustainable conditions for most aerobic organisms in freshwater systems. As concentrations drop below the threshold, conditions become progressively stressful. Minimum oxygen requirements for fisheries in Connecticut's lakes and ponds range from 4 to 5mg/L for cold-water fish (e.g., trout), 2mg/L for cool-water fish (e.g., walleye), and 1 to 2mg/L for warm-water fish (e.g., bass and panfish; Jacobs and O'Donnell 2002).

Temperature, oxygen, and other data were collected from the Amston Lake water column on 13 separate occasions between May 7th and October 20th of 2020 – three more times than in 2019. The additional data collections were made to increase the resolution of temperature and oxygen dynamics in the water column over last year.

Temperature and oxygen data have been displayed as isopleths diagrams where the two variables are shown as shades of colors at each depth throughout the water column and on all dates. The variables between depths and dates where/when measurements were made are interpolated from the actual measurements. Variables of the same value (i.e., color) are connected between dates irrespective of depth to create a theoretical representation of changes at depth over the entire period when data was collected.

A cold and nearly isothermal water column was encountered on May 7th with temperatures at the surface of 13.8°C (56.8°F) decreasing slightly to 11.5°C (52.7°F) at the bottom or approximately 7m of depth. By May 20th and through to June 2nd, a thermocline was detected at approximately 4.5m of depth. By the latter date, a metalimnion was detected with the thermocline acting as the upper boundary, and the lower boundary located one meter below at 5.5m (Fig. 2).

As the temperature in the epilimnetic strata increased, the thermocline descended to 5.5m of depth and an upper boundary to the metalimnion was detected at 4.5m on June 17th.

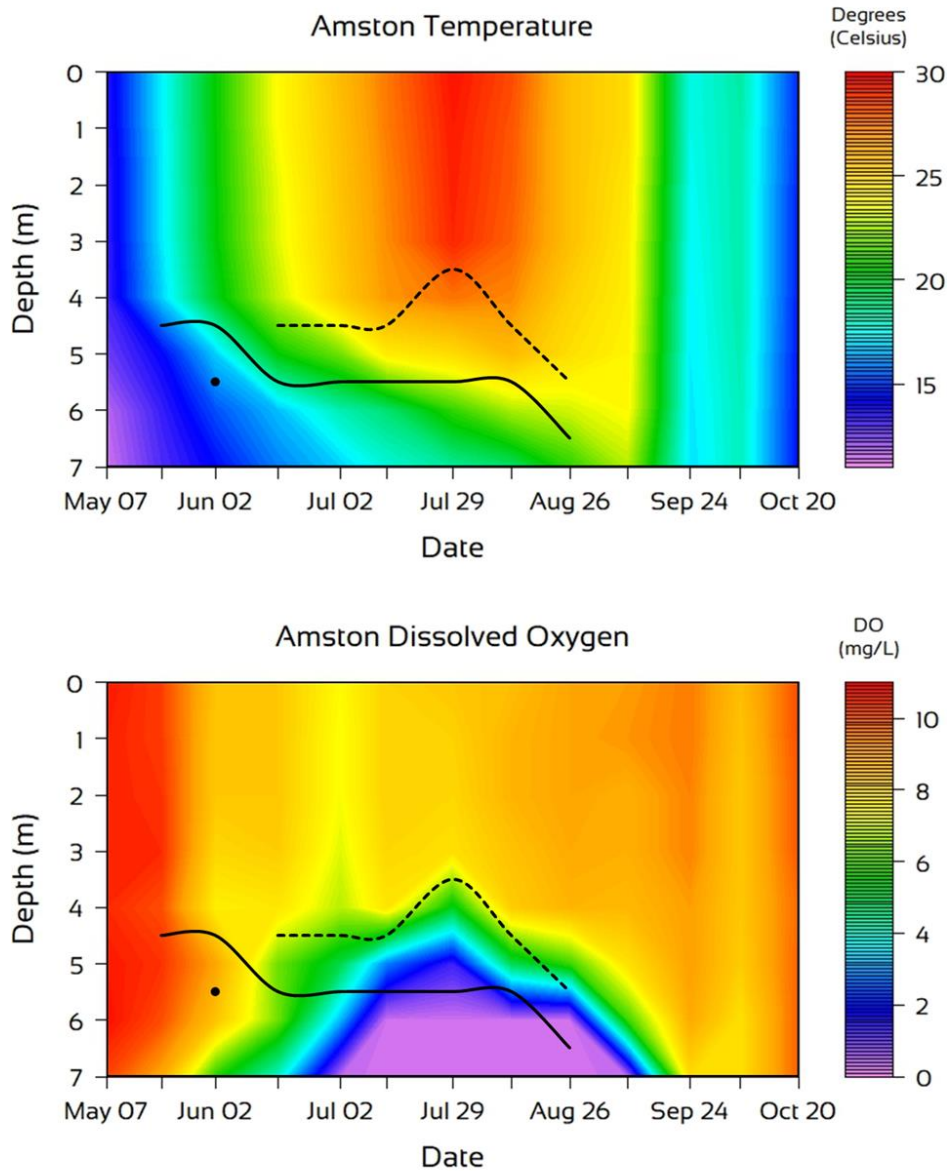


Figure 2. Isopleths of temperature and dissolved oxygen at Amston Lake based on data collected from May 7th through October 20th at one site at Amston Lake. Dashed lines and a single dot represented upper or lower boundaries of the metalimnion. The solid line represents the location of the thermocline.

This pattern of stratification remained constant through July 13th. By July 29th, the upper boundary shifted up a meter while the thermocline remained at 5.5m of depth. Surface temperatures on this date were the warmest recorded in the 2020 season at

29.6°C (85.3°F). Water temperature at the bottom of the water column had increased to 18.6°C (65.5°F) but wouldn't reach their maximum of 22.9°C (72.9°F) until September 9th.

The upper boundary of the metalimnion descended to 5.5m of depth by August 12th, and both the upper boundary and the thermocline descended to 5.5 and 6.5m, respectively, by August 26th. That was the final time stratified conditions were recorded in 2020. By September 9th, temperatures throughout the water were between 24.8 and 22.9°C (76.6 and 72.9°F). Afterwards, the water column became increasingly colder and closer to an isothermal condition (Fig. 2).

Oxygen concentrations of ≥ 10 mg/L were recorded throughout the water column on the two sampling dates in May with one exception. On May 20th, the concentration at the bottom of the water column (~7m of depth) was 9mg/L and represented the first sign of oxygen demand in the sediments exceeding the rate of oxygen replenishment.

In June, concentrations of 8 to 8.5mg/L were measured in the top three meters of the water column, which then decreased with increasing depth except for a metalimnetic oxygen maxima of 9.1mg/L at 5m of depth – which was below the thermocline – on June 2nd (Fig. 2). Possible reasons for this include: the colder temperatures at that stratum, which increases oxygen solubility compared to the warmer temperatures above or a concentrated Cyanobacteria layer generating oxygen via photosynthesis. Concentrations at the bottom of the water column were 5.7 and 4mg/L on June 2nd and June 17th, respectively.

The lowest epilimnetic concentrations of 7.1 to 8.2mg/L occurred in early to mid-July and were concurrent with increased epilimnetic temperatures, which causes oxygen to be less soluble. Oxygen concentrations decreased with depth to < 1 mg/L at the bottom of the water column on July 2nd. The bottom 2m of the water column were < 1 mg/L by July 13th and persisted to August 26th. Epilimnetic oxygen concentrations from July 29th through August 26th increased, which was likely due to wind driven mixing of that strata.

By September 9th, oxygen concentrations were > 5 mg/L through the top 6m of the water column but still < 1 mg/L at 7m of depth. By September 24th, a concentration of ≥ 8 mg/L were measured throughout the mixed water column. After a small decrease in oxygen throughout much of the water column on October 16th, concentrations of ≥ 9.8 mg/L were observed throughout the water column on October 20th.

NUTRIENTS

Total Phosphorus

Phosphorus in freshwater systems is commonly the nutrient in the shortest supply and in greatest demand by the algae; therefore, it is often the nutrient limiting algal productivity. Phosphorus can be imported from the watershed or derived internally from anoxic sediments. Total phosphorus is the analysis most frequently conducted; it represents all forms of phosphorus in a sample, i.e., particulate and soluble forms.

Total phosphorus concentrations in the epilimnion were generally low (Fig. 3). The season average was 11.4µg/L, the season high of 23µg/L occurred on May 7th, and the low of 0µg/L (below detectable limits) was measured on July 2nd and August 26th. The lowest detectable level of 11µg/L was from October 20th. All other epilimnetic concentrations were between 14 and 16µg/L.

Concentration in the metalimnion or middle strata of the water column were measured on dates when the lake was stratified, i.e., May 20th through August 26th and on the first sampling date of the season, May 7th, when the lake was not stratified. As observed in the epilimnion, the highest mid-depth concentration (28µg/L) occurred on May 7th. Unlike in the epilimnion, the August 26th metalimnetic concentration was also relatively high (Fig. 3). The metalimnetic low of 11µg/L was measured on June 2nd. All other concentrations were between 17 and 20µg/L, and the average for the season was 19.8µg/L.

The average hypolimnetic total phosphorus concentration was 30.6µg/L, which included a 0µg/L (below detectable limits) measurement on October 20th. The hypolimnetic average was not significantly higher than those for the epilimnion and metalimnion ($p>0.05$). Concentrations between May 7th and July 2nd were between 17 and 20µg/L. By the end of July, concentrations more than tripled, and by late August were nearly 4X higher than those measured on July 2nd (Fig. 3). Following the breakdown of stratification and subsequent mixing, concentrations decreased to 14µg/L by September 24th, and as noted earlier, were below detectable limits on October 20th.

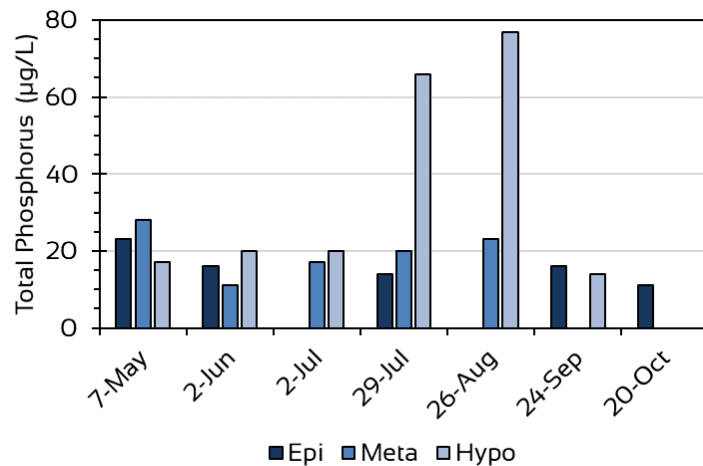


Figure 3. Epilimnetic (Epi), metalimnetic (Meta), and hypolimnetic (Hypo) total phosphorus concentrations at Amston Lake in 2020.

Nitrogen

Nitrogen is regularly the second most limiting nutrient for algae growth in freshwater systems. It can be present in a number of forms in lake water. Ammonia – a reduced form of nitrogen – is important because it can affect the productivity, diversity, and dynamics of the algal and plant communities. The buildup of ammonia can be indicative of internal nutrient loading since bacteria will utilize other forms of nitrogen (e.g., nitrite and nitrate) in lieu of oxygen for cellular respiration under anoxic conditions, resulting in ammonia enrichment of the hypolimnion.

Total Kjeldahl nitrogen (aka TKN) is a measure of the reduced forms of nitrogen (including ammonia) and total organic proteins in the water column. Since TKN accounts for biologically derived, nitrogen-rich proteins in the water column, it is useful in assessing the productivity of the lentic system. Nitrate and nitrite are often below detectable levels in natural systems because they are quickly cycled by bacteria and aquatic plants. Total nitrogen is the sum total of TKN, nitrate, and nitrite. Since the latter two are often below detectable limits, TKN levels are often similar or equal to total nitrogen levels.

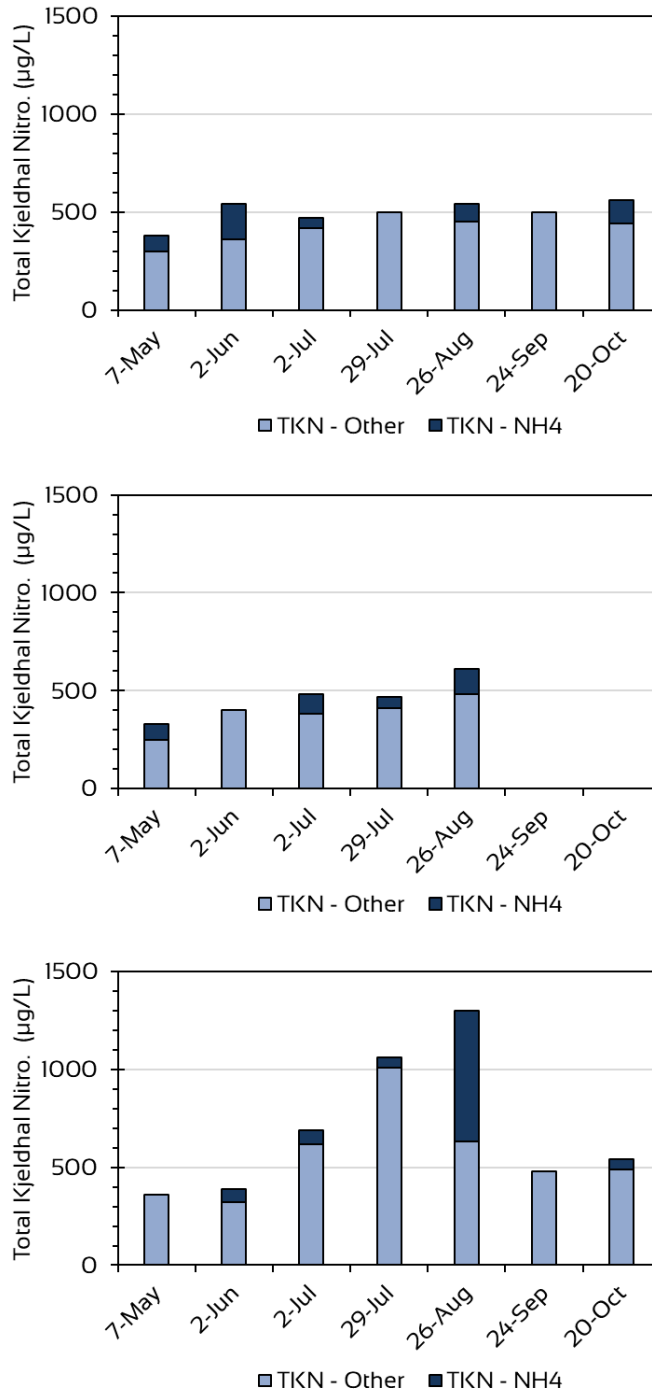


Figure 4. Total Kjeldahl nitrogen (Nitro.) concentrations in 2020 fractionated into ammonia (NH₄) and other constituents in the epilimnion (top panel), metalimnion (middle panel) and hypolimnion (bottom panel).

Nitrite was not detected in any of the samples collected during the 2020 season regardless of stratum. Nitrate was measured above detection levels only once; it was measured in the epilimnetic sample collected on July 2nd and was 150µg/L.

The 2020 average TKN in the epilimnion was 499µg/L. The low for the season was from May 7th at 380µg/L. All other epilimnetic concentrations were between 470 and 560µg/L, the latter being found in a sample from October 20th. Ammonia was regularly a measurable portion of TKN in the epilimnion with the highest percentage (33%; 180µg/L) observed in the June 2nd sample (Fig. 4).

Samples for metalimnetic nitrogen were collected prior to stratification on May 7th and while the lake was stratified (June 2nd through August 26th). The average metalimnetic TKN of 458µg/L was not significantly different than the epilimnetic average ($p>0.05$). Ammonia was almost always a measurable constituent of TKN in this stratum, and had a very similar range as that observed in the epilimnion (Fig. 4.).

As in the epilimnion, hypolimnetic TKN and ammonia was measured on each sampling event ($n=7$). The range of TKN concentrations in the hypolimnion (360 to 1,300µg/L) was larger than in the other strata and this stratum had the highest average of 689µg/L. However, the hypolimnion's TKN concentration was not significantly different than those in the other strata ($p>0.05$). Hypolimnetic concentrations increased from June 2nd through August 26th (Fig. 3). It was on the latter date when ammonia constituted 52% (670µg/L) of total TKN. Following mixing of the water column, hypolimnetic concentrations of TKN and ammonia in September and October decreased; in those months those variables were similar to in concentration to samples collected at 1m of depth.

TN:TP Ratio

Limnologists frequently use the Redfield ratio of 16 (16:1 of nitrogen to phosphorus) to determine whether nitrogen or phosphorus is limiting in a freshwater system (Redfield 1958). The ratio is molar based and when converted to mass, 7.2µg/L is the threshold and when values are less that indicates nitrogen limitation while ratios above 7.2µg/L indicate phosphorus limitations. The Redfield ratios were calculated at all depths for samples collected in May through October.

Table 2. Redfield ratios in the epilimnion (Epi), metalimnion (Meta), and hypolimnion (Hypo) in 2020.

Date	Epi	Meta	Hypo
7-May	16.5	11.8	21.2
2-Jun	33.8	36.4	19.5
2-Jul		28.2	34.5
29-Jul	35.7	23.5	16.1
26-Aug		26.5	16.9
24-Sep	31.3		34.3
20-Oct	50.9		

All ratios, regardless of date or depth, were indicative of phosphorus limitation. In several incidences, “no values” were listed in Table 2 (e.g., epilimnion on July 2nd); “no values” were provided because phosphorus levels were below detection limits and AER reported them as zero. In those instances, nitrogen was detected suggesting phosphorus limitation at the dates and depths that were left blank in Table 2.

SECCHI TRANSPARENCY AND CHLOROPHYLL-A

Secchi disk transparency is a measure of how much light is transmitted through the water column. That transmission is influenced by a number of variables including the amounts of inorganic and organic particulate material in the water column that absorbs or reflects light. In the open water environment, Secchi disk transparency is inversely related to algal productivity, i.e., the more algae in the water, the less Secchi transparency is; and less algal productivity results in greater Secchi transparency. A surrogate measurement of algal productivity is chlorophyll-*a* concentration since it is the photosynthetic pigment common to all freshwater algae, including Cyanobacteria, and representative of algal biovolume.

Light in lakes is important for several reasons including its impact on pelagic photosynthesis and algal growth. As light diminishes with depth, so too does maximum photosynthetic activity. As photosynthesis decreases, there eventually is a stratum where oxygen production from photosynthesis equals oxygen consumed via respiration. That is referred as the compensation depth; it is estimated by multiplying the Secchi disk transparency by 2.

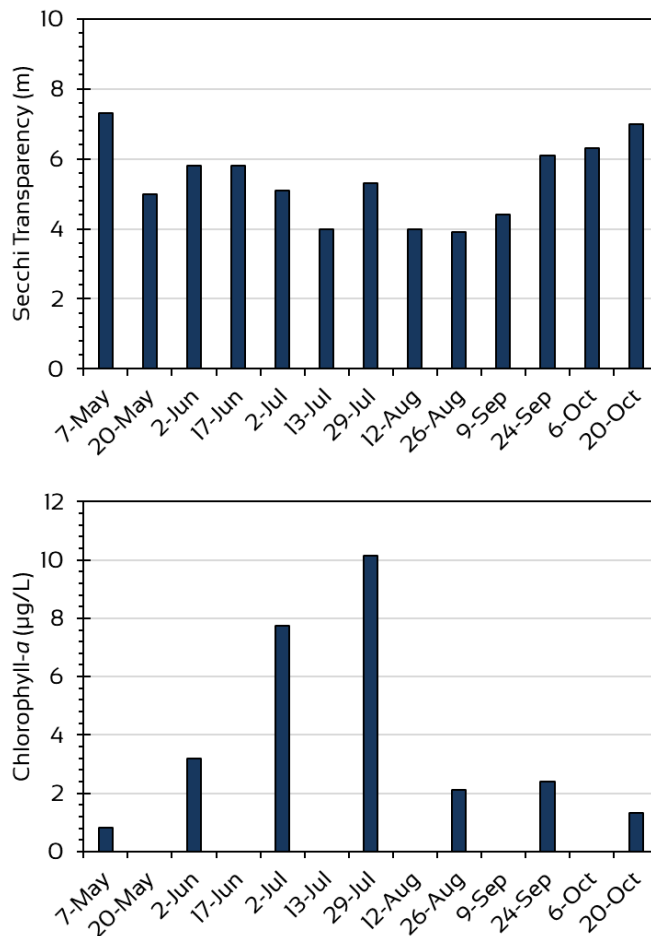


Figure 5. Secchi transparency (top panel) and chlorophyll-a concentrations (bottom panel) measured in Amston Lake in 2020.

Secchi Disk Transparency

Secchi disk transparency was measured 13 times in 2020. The average for the season was 5.38; the maximum values of 7.3 and 7m occurred at the beginning and end of the season. The minimum values of 3.9 to 4.4m occurred from mid-July through early September (Fig. 5).

Transparency generally decreased from May 7th through August 26, before increasing again by October 20th (Fig. 5). The May 7th and October 20th readings were likely underestimated since they were reported as the same length as the depth of the water column.

Chlorophyll-a Concentrations

Chlorophyll-a was measured seven times in 2020. The season average was 3.96µg/L. The season low of 0.82µg/L occurred on May 7th. That progressively increased to a season maximum of 10.15µg/L on July 29th. Concentrations measured in August through September were similar and lower, ranging from 1.3 to 2.5µg/L (Fig. 5).

ALKALINITY AND PH

Alkalinity is a measure of calcium carbonate, and reflects the acid neutralizing capacity of water (i.e., buffering capacity). Alkalinity of surface waters is largely influenced by local geology and other watershed characteristics. Alkalinity at the bottom of the water column can also be generated internally from the biologically mediated reduction of iron, manganese, and sulfate via cellular respiration in the anoxic lake sediments, and denitrification of nitrate to elemental nitrogen (Wetzel 2001).

Epilimnetic alkalinity, and metalimnetic alkalinity when measured (May 7th through Aug 26th) were similar with season averages of 15.7 and 15.8mg/L, respectively. Both trended up as the season progressed (Fig. 6) peaking on August 26th at

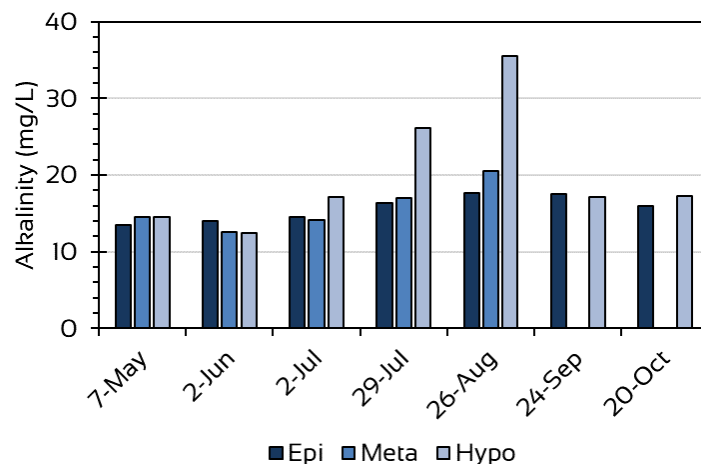


Figure 6. Epilimnetic (Epi), metalimnetic (Meta), and hypolimnetic (Hypo) alkalinity at Amston Lake in 2020.

17.7 and 20.6mg/L, respectively.

Hypolimnetic alkalinity levels were similar to epilimnetic and metalimnetic levels on May 7th and June 2nd (Fig. 6). By July 2nd, hypolimnetic levels started to increase above those at the other strata with concentration differences most pronounced on August 26th when the maximum hypolimnetic concentration of 35.5mg/L was measured. Afterwards epilimnetic and hypolimnetic levels were all between 16 and 17.6mg/L. The hypolimnetic average for the season was 20.0mg/L.

The pH of lake water is important for several reasons. Firstly, very low or very high pH levels will not support diverse lentic fauna and flora. Algal communities are influenced by pH due – in part – to the forms of dissolved carbon in the water column. For example, at pH greater than 8.3, bicarbonate is the dominant form of carbon available to the pelagic algal community; the blue-green algae have adaptive advantages over other algal groups under those conditions because they are able to efficiently utilize that form of carbon. Other algal groups are dependent upon carbon dioxide, which becomes limited in water above pH of 8.3.

The 2020 epilimnetic, metalimnetic, and hypolimnetic average pH levels were 7.2, 6.9, and 6.8, respectively. Levels differed very little among the three strata on May 7th. Epilimnetic levels remained generally constant through July 2nd while pH at lower depths decreased (Fig. 7). Epilimnetic pH levels increased up to 7.7 by August 26th while pH at lower depths remained similar. On September 24th and October 20th, pH in the water column was between 7 and 7.2.

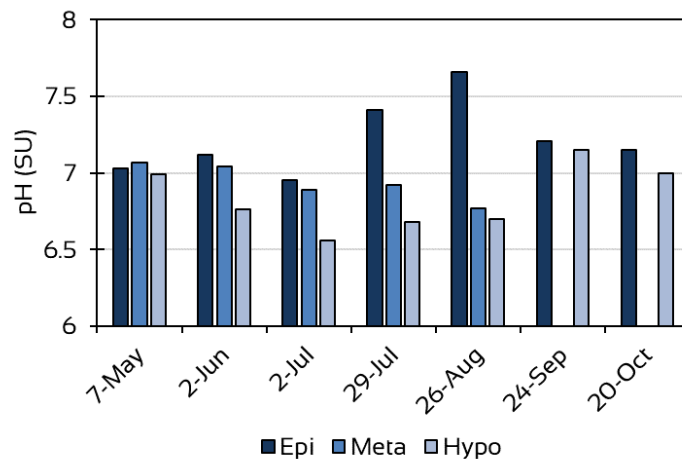


Figure 7. Epilimnetic (Epi), metalimnetic (Meta), and hypolimnetic (Hypo) pH at Amston Lake in 2020.

On August 26th, epilimnetic, metalimnetic, and hypolimnetic pH were measured at 7.7, 6.8, and 6.7, respectively. The epilimnetic pH decreased and hypolimnetic pH increased by September 24th with levels of approximately 7.2 measured at both strata (Fig. 6). Similar levels were observed on October 20th when epilimnetic and hypolimnetic pH levels were approximately 7.2 and 7.0, respectively.

SPECIFIC CONDUCTANCE AND TOTAL DISSOLVED SOLIDS

Conductivity is a surrogate measurement of the dissolved salts or ion concentration in water; as the name suggests, it is a measure of water's ability to conduct an electrical current. Data collection begins with a measure of conductivity. That datum is converted to specific conductance by mathematically standardizing it to a set water temperature (e.g., 25°C) because – in the field – temperature varies with depth and/or date and alters the ability of water to conduct an electrical current.

Specific conductance is an important metric in Limnological studies due to its ability to detect pollutants and/or nutrient loadings. Specific conductance can also have an influence on organisms that inhabit a lake or pond; particularly, algae. The composition of algal communities has been shown to be related, in part, to conductivity levels in lakes (e.g., Siver 1993, McMaster & Schindler 2005).

Specific conductance near the lake bottom sediments can be higher than in regions of the water column nearer the surface; particularly, later in the summer after the water column has been stratified and the waters near the bottom have been anoxic for protracted periods of time. Under those conditions, minerals and salts in the sediments can undergo chemical transformation and change from a particulate state to a dissolved ionic state, diffuse to the waters above the sediments, and increase the conductivity of the hypolimnion.

Total Dissolved Solids (TDS) is a closely related water quality parameter that refers to the amounts of substances that have been dissolved in the water. These substances can include salts, minerals, metals, and other compounds, which can be both organic and inorganic in nature. In their dissolved ionic states, the concentrations of the dissolved solids will determine the levels of resistance to or conductance of electrical flow in water (i.e., conductivity measured as $\mu\text{Siemens/cm}$ or $\mu\text{S/cm}$).

Average specific conductance of the epilimnion, metalimnion, and hypolimnion

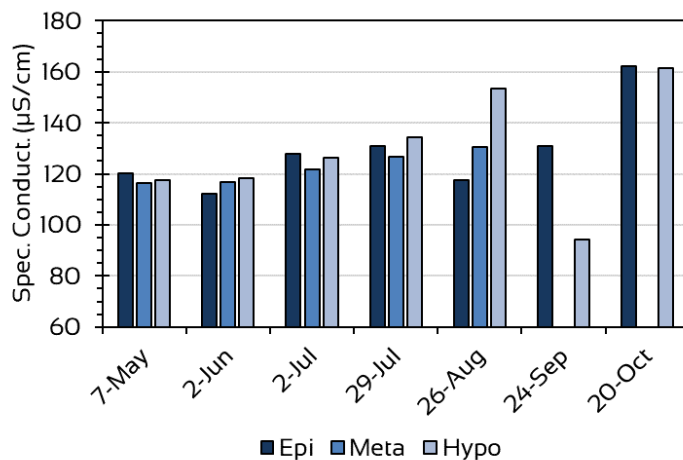


Figure 8. Epilimnetic (Epi), metalimnetic (Meta), and hypolimnetic (Hypo) specific conductance at Amston Lake in 2020.

were not significantly different ($p>0.05$); were 129, 122, and 129 $\mu\text{S}/\text{cm}$, respectively. Measurements at the three strata were similar on each data between May 7th and July 29th and gradually increased over that period of time. On August 24th, levels at the three strata became more discrete with measurements increasing with depth (Fig. 8).

Following mixing of the water column after August 24th, specific conductance continued to gradually increase until they reach their highest levels of 162 $\mu\text{S}/\text{cm}$ on October 20th. The one exception was on September 24th at the bottom of the water column where the lowest specific conductance measurement was reported at 94 $\mu\text{S}/\text{cm}$. We believe this measurement may be in error as a mixed water column typically exhibits similar levels at all depths as observed on October 20th.

As expected, a similar seasonal pattern was observed for total dissolved solids in the Amston Lake water column (Fig. 9). Averages for the epilimnion, metalimnion, and hypolimnion were 91, 87, and 92mg/L, respectively, and differences were not significant ($p>0.05$). The highest concentrations of 115mg/L were from October 20th; the lowest measurement of 67mg/L was from the bottom of the water column on September 24th and potentially erroneous.

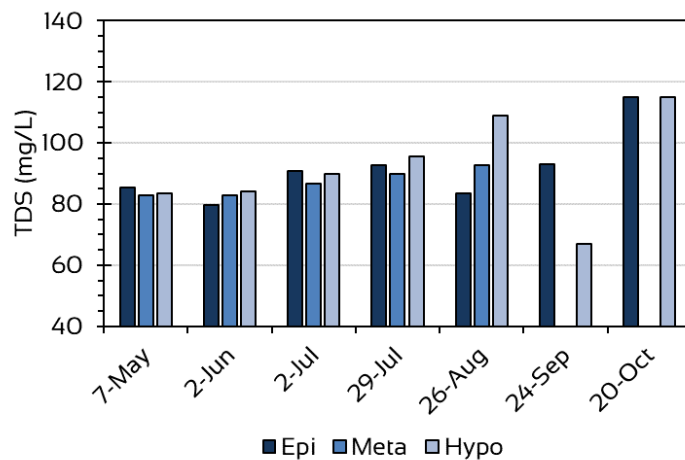


Figure 9. Epilimnetic (Epi), metalimnetic (Meta), and hypolimnetic (Hypo) total dissolved solids (TDS) at Amston Lake in 2020.

CATION AND ANION CONCENTRATIONS

Base cation and anion concentrations are important in understanding natural influences (e.g., dissolved salts from bedrock geology) as well as anthropogenic influences in the watershed (e.g., road salts). In most lakes, the dominant base cations in lake waters are calcium (Ca^{2+}), magnesium (Mg^{2+}), sodium (Na^+) and potassium (K^+). Dominant anions include chloride (Cl^-), sulfate (SO_4^{2-}), and the alkalinity ions – carbonate (CO_3^{2-}), and bicarbonate (HCO_3^-). Those cations and anions are derived, in part, from total dissolved solids and collectively contribute to conductivity levels in lake water. The ratios of different ions can be diagnostic when compared to other lakes, and when compared to levels in the same lake over time.

Table 3. Summary statistics for base cation and anions measured in epilimnetic samples collected from Amston Lake in 2020. Avg = average; St Dev = standard deviation; Ca²⁺ = calcium; Mg²⁺ = magnesium; K⁺ = potassium; Na⁺ = sodium; Cl⁻ = chloride; Alk = alkalinity anions.

Unit	Statistic	Ca ²⁺	Mg ²⁺	K ⁺	Na ⁺	Cl ⁻	Alk
mg/L	Avg	7.19	1.55	1.80	13.50	22.23	16.02
	St Dev	0.18	0.07	0.00	0.40	1.34	1.54
meq/L	Avg	0.36	0.13	0.05	0.59	0.64	0.32
	St Dev	0.01	0.01	0.00	0.02	0.04	0.03

We reported monthly base cations, chloride, and the alkalinity anion data by their mass (mg/L) and by their electrochemical equivalents (meq/L). The latter is performed by dividing the mass of an ion by its equivalent weight which provides for an accounting of the amount of electric charge (positive or negative). Summary data are provided in Table 3.

In general, base cation and anions in the epilimnion were conservative water quality variables, i.e., there was little variability over the course of the season (Table 3). On a mass (mg/L) and equivalent (meq/L) basis, sodium followed by calcium were the most prevalent cations. Chloride and the alkalinity anions were each greater in mass than any of the cations.

Solutions, including lake water, are electrically neutral, i.e., the sum of positive charge from the cations equals the sum of the negative charge of the anions. The average sums of cations and anions on a meq/L basis (which factors in electrical change) were 1.12 and 0.97meq/L, respectively. The other major anion in lake water not measured here is sulfate. Sulfate can be estimated by calculating the difference between the sum of the base cations and the sum of the other anion. Using that formula, we estimate the sulfate concentration to be 0.15meq/L. The average milliequivalents of sodium were similar to that of chloride (Fig. 10).

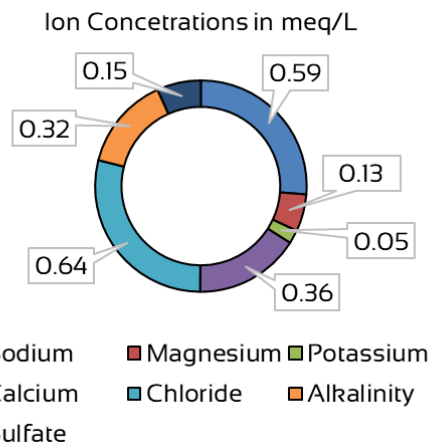


Figure 10. Average concentrations of base cations, chloride, and alkalinity measured in 2020. Sulfate was estimated by subtraction.

Likewise, calcium and alkalinity levels were similar, as were magnesium and sulfate concentrations. Sodium chloride is a common chemical compound widely used for de-icing roads in the winter. Calcium carbonate is found naturally in lake water and is the chemical compound that is measured in assessments of alkalinity. Magnesium sulfate is a chemical compound used in agriculture for soils that are deficient in magnesium, which is an essential nutrient for plants.

ALGAL DYNAMICS

Qualitative and quantitative analyses of the algal community have been important components of lake water quality studies for many years. Algae as bioindicators can provide insight into levels of nutrients and other chemical characteristics of lake water. They are responsive to reductions as well as improvements to water quality. In recent years, analyses have focused on toxigenic Cyanobacteria in freshwaters due to the threat they pose to human and pet health when their concentrations are high.

Forty-five different algal genera were identified in the phytoplankton net or whole water samples and were asymmetrically distributed among six taxonomic groups (Appendix A). Two-thirds of those genera were from two taxonomic groups. The Chlorophyta (aka Green Algae) were represented by 21 different genera. The number of Cyanobacteria (aka Blue-green Algae) genera identified was 11. Bacillariophyta (aka Diatoms), Chrysophyta (aka Golden Algae), Pyrrophyta (aka Dinoflagellates), and Euglenophyta were collectively representative of 13 genera.

Cell count data was utilized to assess the pelagic algal community two ways. First, cell concentrations for each genus, for the six taxonomic groups, and the total community were determined for each sample (Fig. 11a). Relative abundance based on cell concentrations were also determine (Fig. 11b). Cell concentrations were generally low with the lowest levels of $>1,350$ cells/mL in samples collected on May 7th and June 2nd. Important taxa in these early season samples included Chlorophyta, Chrysophyta, and Cyanobacteria. Concentrations increased to a maximum of 6,236 cell/mL by July 29th and were co-dominated by Chlorophyta and Cyanobacteria (Fig. 11b). Chlorophyta concentrations decreased and Cyanobacteria cell concentrations increased afterwards and until the end of the season.

The second way the algal community was assessed was by biovolume which accounted for the diverse cell sizes and shapes that are encountered in the algal community. Estimates of cell biovolume were performed by applying standard volume calculations for geometric shapes that were similar to algal shapes (e.g., spheres, cylinders, cuboids) and average cell dimension observed for the genera. Estimated biovolumes for each taxon and the community are presented in Fig. 11c and relative biovolume as a percent of the total is presented in Fig. 11d.

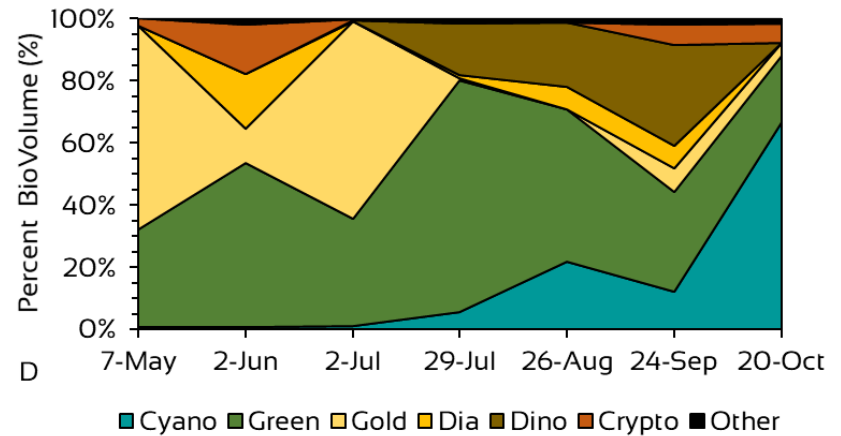
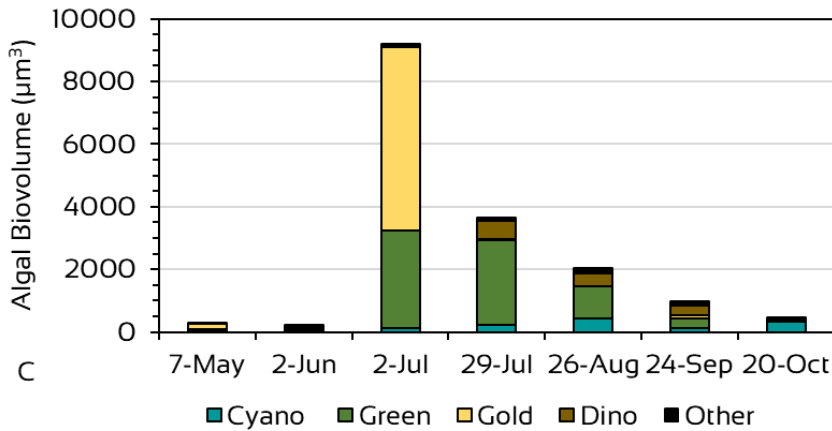
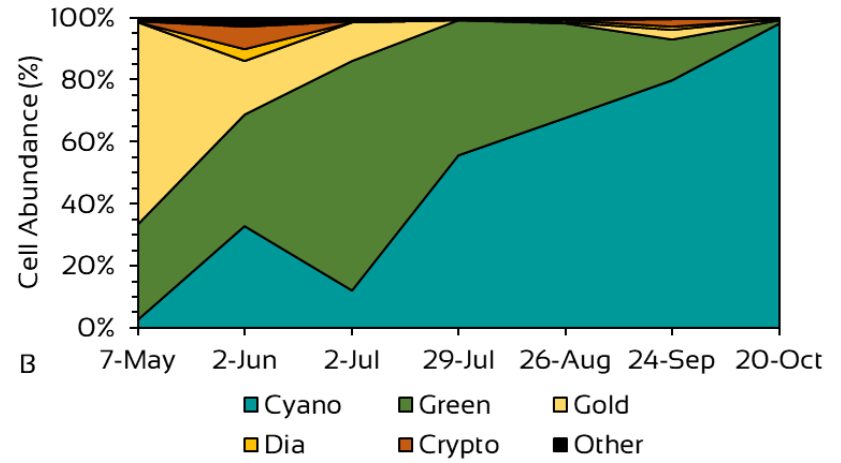
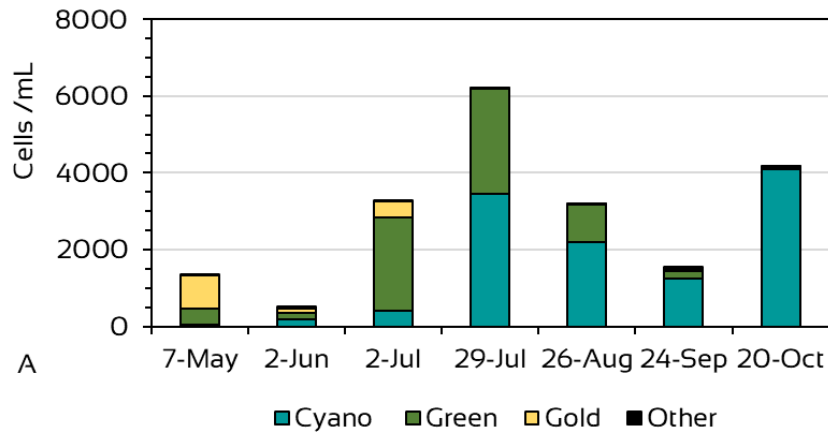


Figure II. A – algal cell concentrations by taxa and date; B – relative abundances of cells by taxonomic group and date; C – algal biovolume by taxonomic group and date; and D – percent biomass by taxonomic group and date. Cyanobacteria = Cyano, Green = Green Algae or Chlorophyta, Gold = Golden Algae or Chrysophyta, Dia = Diatom or Bacillariophyta, Dino = Dinoflagellate or Pyrrhophyta, Crypto = Cryptophyta

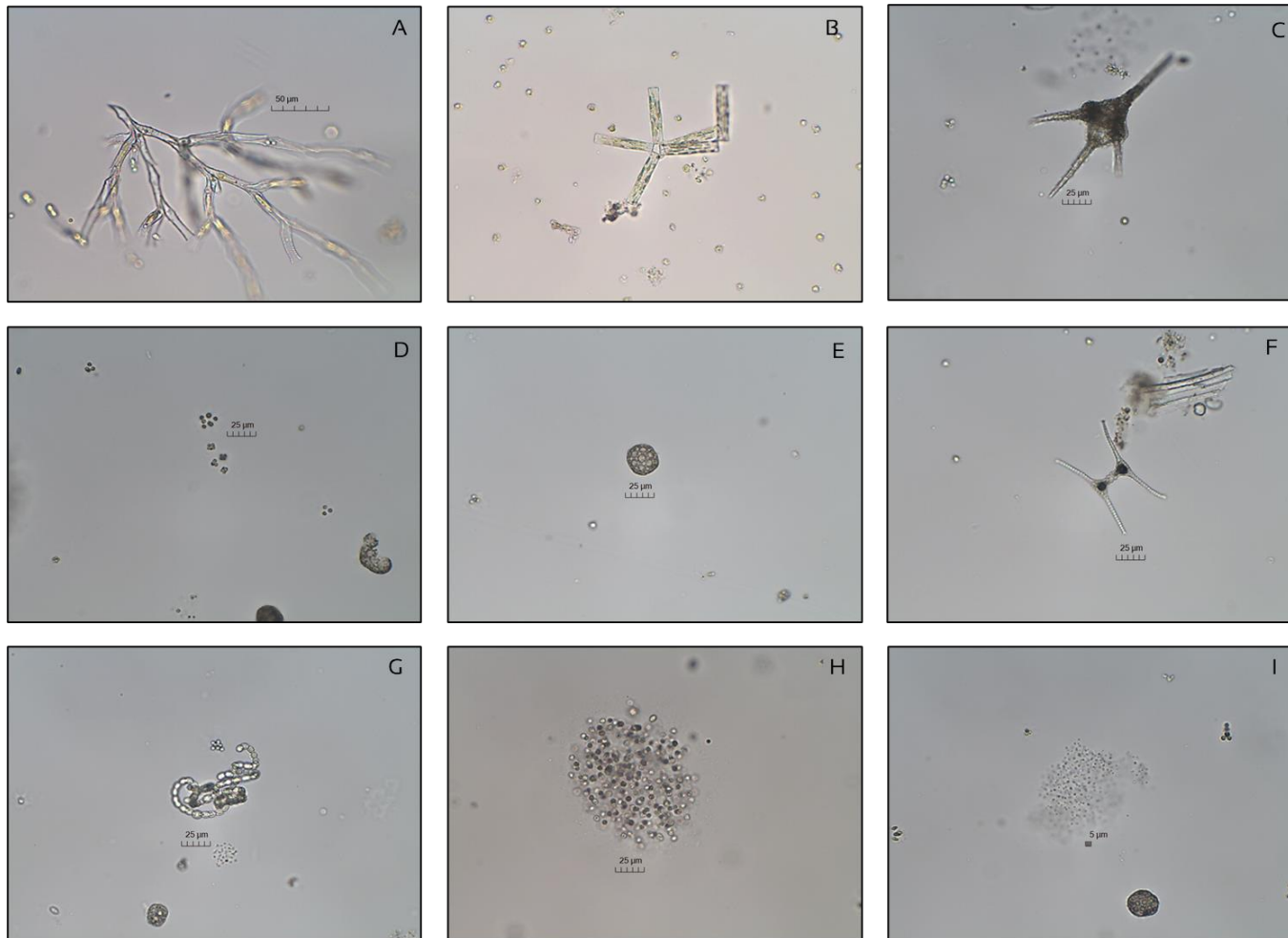


Figure 12. Micrographs of algae specimens taken from Amston Lake samples in 2020. A. The Golden Algae *Dinobryon* spp.; B. the Diatom *Tabellaria* spp.; C. the Dinoflagellate *Ceratum* spp.; the Green Algae D. *Gloeocystis* spp., E. *Coelastrum* spp., and F. *Staurastrum* spp.; the Cyanobacteria G. *Dolichospermum* spp., H. *Microcystis* spp., and I. *Aphanocapsa* spp.

Low cell concentrations and the small sizes of the genera counted on May 7th and June 2nd, which were mostly from the Chlorophyta and Chrysophyta, yielded the lowest biovolumes. The maximum biovolume of 9,199 $\mu\text{m}^3/\text{mL}$ occurred on July 2nd and was due to the season's highest concentration of the Chrysophyta genus *Dinobryon spp.* (Fig. 12a), which form dendritic colonies with relatively large cells. Chlorophyta, principally *Gloeocystis spp.* (Fig. 12d), also comprised a large part of the biovolume. By July 29th, Chrysophyta were nearly absent but Chlorophyta continued to maintain the same biovolume and now included the colonial *Coelastrum spp.* (Fig. 12e). Although cell concentrations were low, the biovolume of the Pyrrophyta became important due to the presence of the very large unicellular dinoflagellate *Ceratium spp.* (Fig. 12c).

The total biovolume decreased after July 2nd through October 20th. During that time, the percentage of Cyanobacteria biomass increased to 310 $\mu\text{m}^3/\text{mL}$ or 66.5% of the total. Important Cyanobacteria genera included *Dolichospermum spp.* (Fig. 12g), *Microcystis spp.* (Fig. 12h), and *Aphanocapsa spp.* (Fig. 12i). Regardless of the increased Cyanobacteria biovolume, cell concentrations for the season never exceeded 4,100 cells/mL. The State of Connecticut recommends thresholds of 20,000 and 100,000 Cyanobacteria cells/mL as triggers for mitigation measures in the interest of public health (CT DPH & CT DEEP 2019). Recommended measures after exceeding the first threshold includes posting warning signs at public beaches; after exceeding the second threshold, beach closing signage is recommended.

PUBLIC HEALTH MONITORING

In 2019 and 2020, the Lake Health Committee collected samples from popular recreational areas on shoreline of Amston Lake, and from the shoreline along the North Cove, for analyses of total coliform and *Escherichia coli* (*E. coli*). Total coliform is ubiquitous and generally harmless (CT DPH 2010). The State of Connecticut use *E. coli* as the indicator organism for sanitary water quality at freshwater beaches since it is naturally found in large quantities in the intestines of people and warm-blooded animals. Acceptable concentrations at public beaches are ≤ 235 organisms per 100mL.

On November 20, 2019, results from samples collected at eight sites ranged from <10 to 52 organisms per 100mL, were all below the State's threshold, and indicative of good sanitary water quality conditions. Results from five of the eight samples were ≤ 20 organisms per 100 mL. The highest concentrations (41 to 52 organisms per 100 mL) were from samples collected in the North Cove.

On July 20, 2020 another set of samples were collected at the same locations. All results were reported as 10 or <10 organisms per 100 mL and characteristic of good sanitary water conditions (CT DPH 2016).

2020 LAKE WATER QUALITY ASSESSMENT

Trophic Status

A lake's trophic state or status is an account of the level of productivity, particularly open water algal productivity, that a lake supports. Average summer chlorophyll-*a* concentration and Secchi disk transparency provide direct measures of productivity and are used in conjunction with the average levels of nutrients that can limit algal productivity (i.e., total phosphorus and total nitrogen). Table 4 provides a standard framework of how those variables are used to assess trophic status developed in Connecticut.

Amston Lake average Secchi disk transparency in 2020 was 5.38m. The average transparency based on measurements taken from June through August was 4.84m. In both instances, average Secchi disk transparency was within the early mesotrophic range.

The season average chlorophyll-*a* concentration was 3.9 $\mu\text{g/L}$ and also characteristic of early mesotrophic productivity. The average based on measurements from June through August (5.8 $\mu\text{g/L}$) did fall within the low end of the mesotrophic range (Table 4). Algal productivity does increase in lakes during the summer months as was reflected in the Secchi and chlorophyll-*a* concentrations at Amston Lake.

The average epilimnetic total phosphorus concentration at Amston Lake was 11.4 $\mu\text{g/L}$ and characteristic of early mesotrophic productivity. The season averages increased with depth with the greatest average of 30.6 $\mu\text{g/L}$ in the hypolimnion, which could support productivity commensurate with eutrophic conditions. Hypolimnetic concentra-

Table 4 . Trophic classification criteria used by the Connecticut Experimental Agricultural Station (Frink and Norvell 1984) and the CT DEP (1991) to assess the trophic status of Connecticut lakes. The categories range from oligotrophic or least productive to highly eutrophic or most productive.

Trophic Category	Total Phosphorus ($\mu\text{g} / \text{L}$)	Total Nitrogen ($\mu\text{g} / \text{L}$)	Summer Chlorophyll- <i>a</i> ($\mu\text{g} / \text{L}$)	Summer Secchi Disk Transparency (m)
Oligotrophic	0 - 10	0 - 200	0 - 2	>6
Early Mesotrophic	10 - 15	200 - 300	2 - 5	4 - 6
Mesotrophic	15 - 25	300 - 500	5 - 10	3 - 4
Late Mesotrophic	25 - 30	500 - 600	10 - 15	2 - 3
Eutrophic	30 - 50	600 - 1000	15 - 30	1 - 2
Highly Eutrophic	> 50	> 1000	> 30	0 - 1

tions diverged from epilimnetic and metalimnetic concentrations on July 29th and August 26th and were of levels capable of supporting highly eutrophic productivity (Fig. 2, Table 4).

These season high hypolimnetic total phosphorus levels were concurrent with protracted periods of anoxia below 6m of depth implicating autochthonous sources, i.e., derived from the sediment within the lake itself. The Compensation Depth (that theoretical depth where oxygen generated by photosynthesis equals oxygen consumed in cellular respiration) was always greater than the total depth at the sampling site, and implies that the anoxic conditions near the bottom were due to the oxygen demand in the sediments.

The average total nitrogen concentration in the epilimnion was 520µg/L and within the late mesotrophic range. On five of the seven dates when samples were collected for nitrogen analyses, ammonia was measured in the epilimnion. Detectable levels of ammonia in the epilimnion are typically not common since ammonia is quickly assimilated by plants and algae.

At Amston Lake, phosphorus is the limiting nutrient (Table 2) so an early mesotrophic designation is appropriate in light of the other trophic variables. The higher nitrogen levels may contribute to the competitiveness of algal genera from taxa other than Cyanobacteria, e.g., Chlorophyta (aka Green Algae). A number of Cyanobacteria genera can fulfil nitrogen requirements from elemental nitrogen from the atmosphere that has diffused into the water, including several genera observed at Amston Lake, e.g., *Dolichospermum spp.* and *Microcystis spp.* Genera from other algal taxa cannot.

Ionic Concentrations

There was an approximately 40µS/cm range in epilimnetic specific conductance and an approximately 65µS/cm range in hypolimnetic specific conductance during the course of the season (Fig. 8). A wide range in hypolimnion specific conductance is common and often related to anoxic conditions near the bottom resulting in the transformation of precipitated compounds in the sediments into their soluble forms, thus increasing specific conductance near the bottom. This was exemplified on August 26th when hypolimnetic specific conductance was 36µS/cm greater than the corresponding epilimnetic level (Fig. 8) near the end of a protracted period of anoxic conditions (Fig. 2).

By September 24th the water column was mixed but the hypolimnetic specific conductance was recorded as nearly 37µS/cm lower than that measured in the epilimnion. With a mixed water column, we would anticipate similar specific conductance readings at the top and bottom of the water column and are suspect of that the September 24th hypolimnetic data.

The wide specific conductance range observed in the epilimnion is not common. The October 20th specific conductance in the epilimnion (and in the hypolimnion) was the highest recorded over the last two years. To examine the phenomenon, epilimnetic specific conductance was plotted over the last two years (Fig. 13). All points over that time were within 110 and 132 $\mu\text{S}/\text{cm}$, with the exception of the October 20, 2020 measurement of 162 $\mu\text{S}/\text{cm}$.

Additionally, ion equivalents of the base cations and anions were regressed against the specific conductance over the same period of time (Fig. 14). No compelling relationship was observed that would explain the high reading from October 20, 2020. The analysis did reinforce the relationships between sodium and chloride and between calcium and alkalinity at Amston Lake discussed earlier.

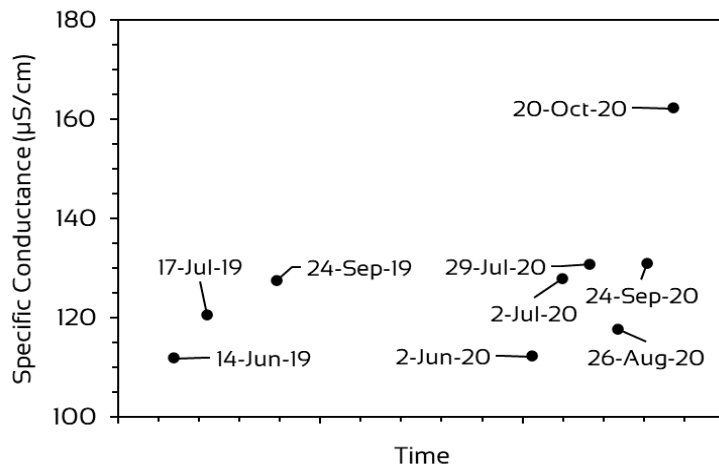


Figure 14. Specific conductance in the epilimnion of Amston Lake over time from June 14, 2019 to October 20, 2020

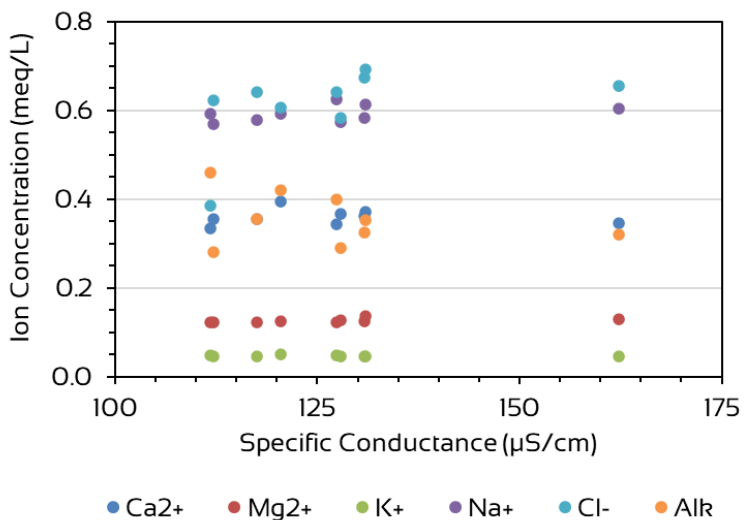


Figure 13. Ion concentrations of the based cations, chloride and alkalinity regressed against specific conductance measured in the epilimnion from June 14, 2019 to October 20, 2020. Ca²⁺ = calcium; Mg²⁺ = magnesium; K⁺ = potassium, Na⁺ = sodium; Cl⁻ = chloride; and Alk = alkalinity.

STORMWATER

Nutrients

The average total phosphorus concentration based on all stormwater sites on April 9th (393 $\mu\text{g/L}$) was significantly higher ($p < 0.005$) than the May 1st average (38 $\mu\text{g/L}$). The season averages for the Hebron and Lebanon sites (271 and 184 $\mu\text{g/L}$, respectively) were not significantly different ($p > 0.05$). Sites with notably high concentrations on both sampling days were H-4 and L-4 (Fig. 15). Several sites had notably higher concentration on April 9th, but not May 1st; these included H-6, H-13, and L-12. At the L-32 site, the May 1st concentration was greater than the April 9th concentration.

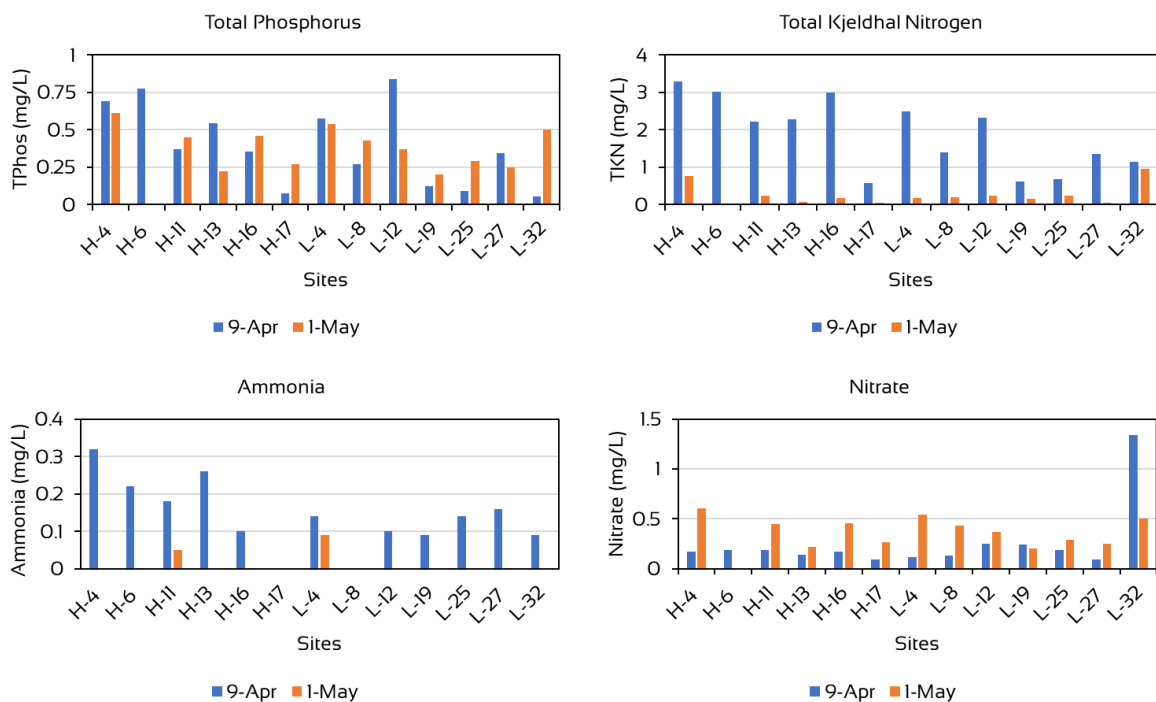


Figure 15. Levels of total phosphorus, total Kjeldahl nitrogen, ammonia, and nitrate in samples collected from six Hebron (H) and seven Lebanon (L) stormwater collection sites on April 9th and May 1st in 2020. Levels are displayed in mg/L. For $\mu\text{g/L}$, multiply mg/L by 1000.

Characteristics of total Kjeldahl nitrogen (TKN) in stormwater samples were similar to those of total phosphorus. The April 9th average based on all sites (1880 $\mu\text{g/L}$) was significantly higher ($p < 0.005$) than the May 1st average (380 $\mu\text{g/L}$). The Hebron sites average (1,490 $\mu\text{g/L}$) was not significantly higher ($p > 0.05$) than the Lebanon sites average (900 $\mu\text{g/L}$). TKN concentrations at five of the six Hebron sites exceeded 2,000 $\mu\text{g/L}$

on April 9th while only two of the seven Lebanon sites exceeded that level on that date. Concentrations on May 1st were between 200 and 610 $\mu\text{g}/\text{L}$, regardless of site.

Ammonia concentrations were measurable in samples from most of the 13 stormwater sites on April 9th, ranging between 90 and 320 $\mu\text{g}/\text{L}$ (Fig. 15). Ammonia was measurable in only two of the 13 sites on May 1st; one site was in Hebron (H-11) and one site in Lebanon (L-4).

Nitrate concentrations tended to be higher on May 1st but the average on that day (0.25mg/L) was not significantly different ($p>0.05$) from the April 9th average (0.27mg/L). Site L-32 exhibited a much higher concentration on April 9th compared to any other sample (Fig. 13). Low levels of nitrites were only detected from samples collected on April 9th from the following sites: H-4, L-4, L-8, and L-12.

Ion concentrations

We assessed concentrations of sodium, potassium, calcium, magnesium, chloride, and alkalinity measured in milliequivalents, as well as specific conductance in $\mu\text{S}/\text{cm}$, from all stormwater sites and from both collection dates in 2020 (Fig. 16). Relationships between variables, dates and site (Hebron sites vs Lebanon sites) were examined.

Average sodium or chloride did not significantly differ by date, and average chloride levels in April 9th samples did not significantly differ from the average of the May 1st samples ($p>0.05$); average chloride from Hebron samples was significantly greater than the Lebanon average (0.52 vs. 0.18meq/L, respectively; $p<0.05$). The H-11, H-13, and H-16 sites exhibited higher concentrations of both ions on both dates; concentrations of both ions were notably high on May 1st at the H-4 site (Fig. 16).

Average specific conductance did not significantly differ based on date or town where sites were located. As with sodium and chloride, specific conductance was generally highest at H-11, H-13, and H-6. Specific conductance at H-4 was also notably high on May 1st. The relationships between specific conductance, sodium, and chloride were the strongest among the ion variables (Fig. 17). The correlation between sodium and chloride was very strong (Fig. 18).

Average calcium and magnesium concentrations did not significantly differ based on the town in which the sample was collected ($p>0.05$). Average calcium concentrations for each collection date did not significantly differ ($p>0.05$); average magnesium on April 9th was significantly higher than the May 1st average ($p<0.05$). The highest concentrations measured in samples from April 9th were from L-12, H-4, H-6, L-4, and L-8 (Fig. 14). Potassium levels followed a pattern similar to magnesium with average April 9th levels significantly higher than the May 1st average ($p<0.05$) but not significantly different based on which town samples were collected in.

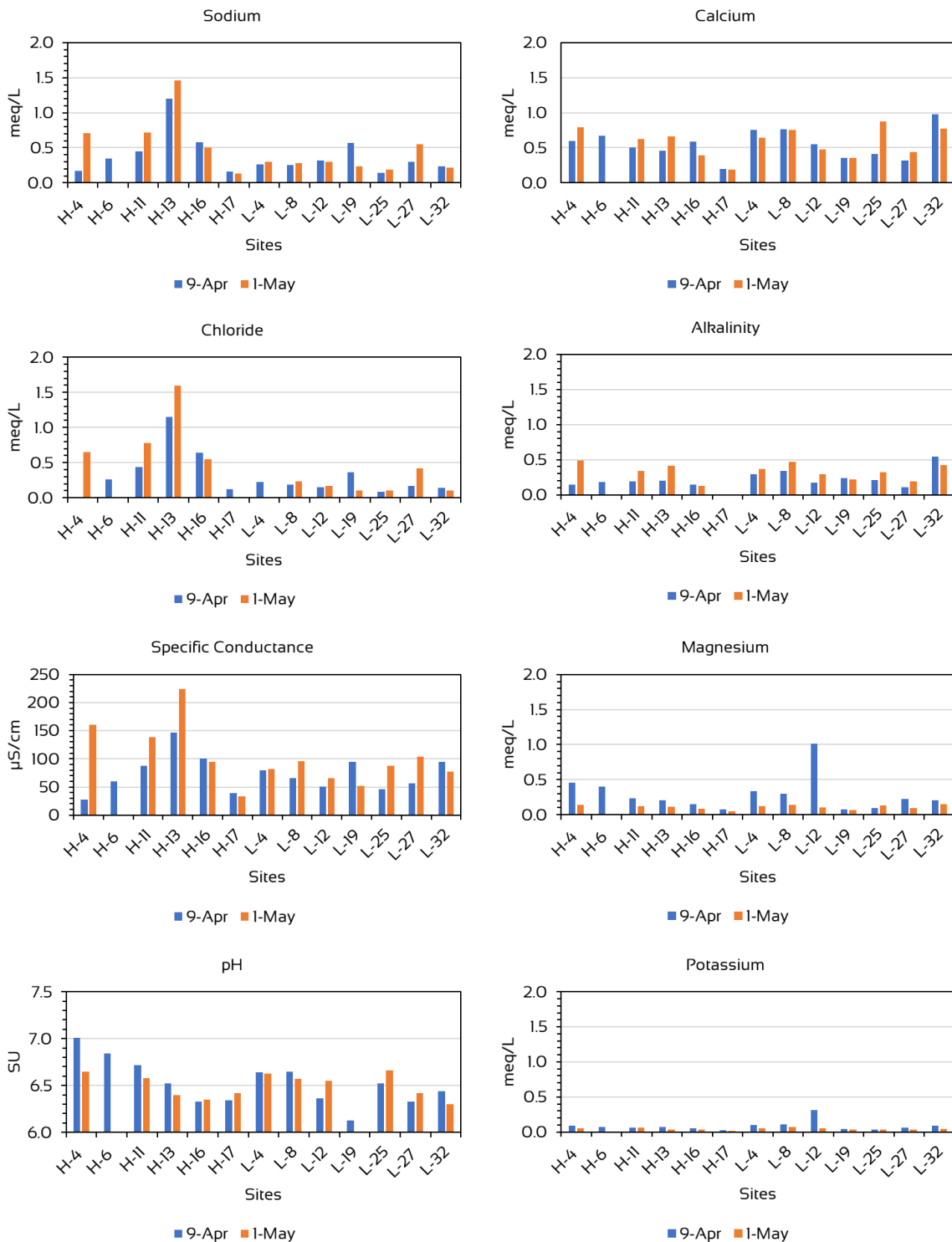


Figure 16. Concentrations of sodium, calcium, chloride, alkalinity, magnesium, and potassium, specific conductance and pH at 13 stormwater quality sites in 2020.

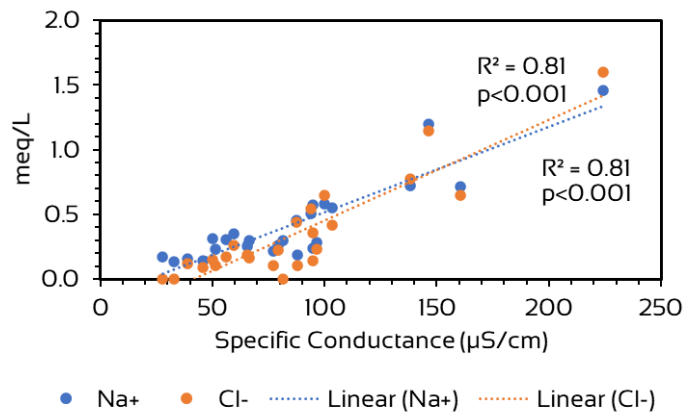


Figure 18. Linear regressions of sodium (Na+) and chloride (Cl-) against specific conductance in samples collected at the stormwater sites at Amston Lake in 2020.

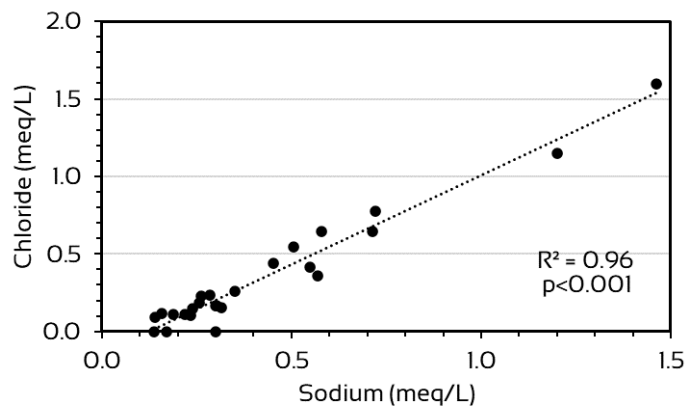


Figure 17. Linear regression of sodium and chloride concentrations in samples collected at all stormwater sites at Amston Lake in 2020.

Average alkalinity did not differ based on date or town samples were collected in. However, there was fair relationship between alkalinity and specific conductance ($r^2 = 0.29$; $p < 0.05$). Average pH values based on sample date and town in which the sample was collected did not significantly differ ($p > 0.05$).

Stormwater Assessment

Amston Lake receives nutrients and other ionic substances in drainage from its watershed. Average total phosphorus and total Kjeldahl nitrogen concentrations were significantly higher in samples collected on April 9th while most of the other ionic variables did not significantly differ based on sampling date. The two exceptions were magnesium and potassium. We graphically displayed concentrations of the ions in stormwater samples on the same scale, i.e., from 0 to 2meq/L for comparative purposes (Fig. 16). Magnesium and potassium levels are relatively low compared to sodium, calcium, or chloride suggesting that much of the watershed sources of magnesium and potassium are exported sooner than the others, e.g., sodium and chloride.

The same principal generally holds true for nutrients. Much of the effort to control watershed/stormwater-borne phosphorus focuses on “first flush” technology or methods that treat the initial volumes of stormwater (e.g., capture and infiltrate) because phosphorus concentrations are typically higher in those volumes. The average phosphorus concentration from the April 9th samples was an order of magnitude greater than the May 1st average (393 vs 38µg/L, respectively) and the May 1st stormwater average was consistent with the May 7th concentration in the lake (average of 22.7µg/L based on analyses at three strata).

Nitrogen levels in April 9th samples were even more disparate than phosphorus levels from corresponding May 1st concentrations. It is unclear why this is. Nitrogen does not adhere to soil particles as well as phosphorus and might be prone to a quicker flushing through the system. The average May 1st stormwater TKN concentration of 380µg/L was very similar to the lake water column average of 357µg/L on May 7th.

There were sites that tended to have higher stormwater phosphorus concentrations than the others. These included H-4, H-6, H-13, L-4, and L-12. The list of sites is slightly larger for TKN (Fig. 15). Analyses of patterns of land use in the specific drainage areas for those sites may aid developing mitigation strategies. For example, if a drainage area was largely residential, then an educational campaign on “Best Management Practices” for homeowners may be warranted. If the dominant land use is large parking lots, then structural measures might be considered.

The general relationship between sodium and chloride, and their relationship with specific conductance implies an impact from deicing road salts. Average chloride concentration from the Hebron stormwater sites was significantly higher than the Lebanon average. Similar assessments of land use in specific drainage basins may aid in developing effective mitigation strategies.

WATER QUALITY TRENDS

Trends in water quality were analyzed using two statistical methods. First, a multiple linear regression (MLR) method was employed to determine if the epilimnion, hypolimnion, and/or the entire lake water column – based on the combination of variables listed in Table 5 – had changed significantly since 1994. A p-value was calculated to determine if the null hypothesis (i.e., numbers are randomly distributed in multidimensional space) was accepted or rejected (i.e., there was a pattern in the data set that differed from random) with $p < 0.05$ indicating the latter. The same statistical method was applied to the stormwater data that extended back to 2001. Stormwater data was analyzed in its entirety, as well as in subsets based on the municipality where the site was located i.e., Hebron or Lebanon.

Table 5. Variables used in Multiple Linear Regression and ANOVA. Spec. Cond. = specific conductance; Total Phos. = total phosphorus

Variable	Lake	Stormwater
Alkalinity	✓	
Ammonia	✓	
Nitrate		✓
pH		
Spec. Cond.	✓	✓
TKN	✓	
Total Phos.*	✓	✓
Turbidity		✓

*Total phosphorus was removed from the lake epilimnetic dataset due to lack of variance

The second analysis performed was analysis of variance or ANOVA. With ANOVA each variable was examined independently to determine whether a change had occurred in a statistically significant manner over time. The F-statistic is used to calculate the probability (i.e., p-value) that a dataset's variable pattern differs from a random distribution of values. ANOVA was performed for the same lake water data groupings (epilimnion, hypolimnion, and combined data) and stormwater data groupings (all sites, Hebron sites, and Lebanon sites).

Lake Trends

Results from MLR indicated that water quality in Amston Lake has significantly changed since 1994. This finding was based on the combined epilimnetic and hypolimnetic dataset (Appendix B). Significant change was not detected when the data from the two strata were analyzed independently. The variables of alkalinity, and to a lesser extent total phosphorus and specific conductance were those contributing the most to the significance of the model.

Based on ANOVA and variables from the combined epilimnetic and hypolimnetic dataset, significantly positive (increasing) changes were detected in concentrations of

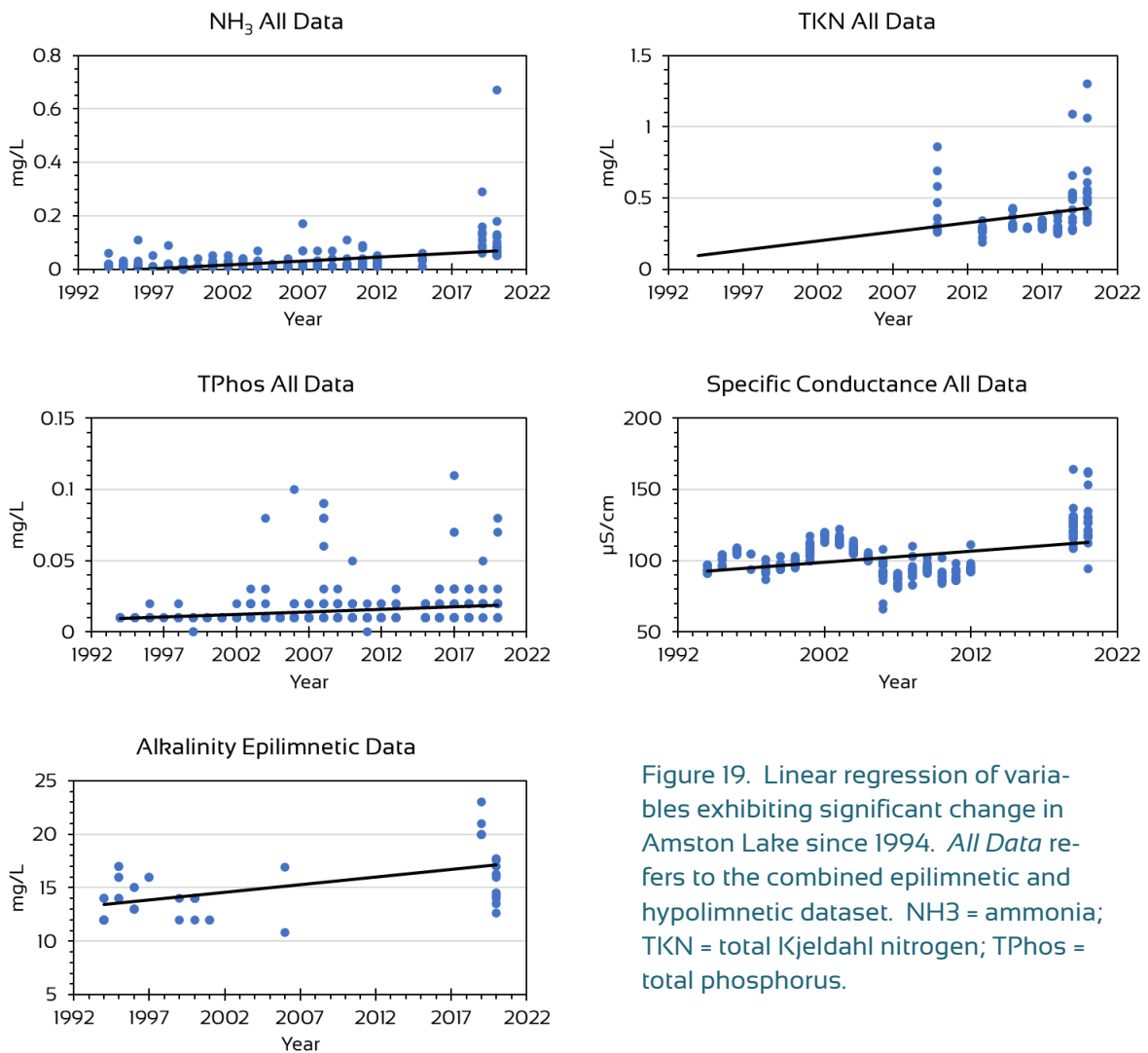


Figure 19. Linear regression of variables exhibiting significant change in Amston Lake since 1994. *All Data* refers to the combined epilimnetic and hypolimnetic dataset. NH₃ = ammonia; TKN = total Kjeldahl nitrogen; TPhos = total phosphorus.

ammonia, total Kjeldahl nitrogen, and total phosphorus. Specific conductance also significantly increased based on this dataset, as did alkalinity based on the epilimnetic data since 1994 (Fig. 19).

Stormwater

MLR analyses also indicated significant change in the chemistry of stormwater entering Amston Lake since 2001 based on the combined Hebron and Lebanon dataset, and on the Hebron and Lebanon sites data utilized independently. For the combined data and the Hebron data, the most important variable contributing to the significance of both models was total phosphorus. The trend was negative (decreasing). For the

Lebanon stormwater sites, the most important variables were nitrate and specific conductance which were both trending in a negative manner.

Results from ANOVA indicated significant negative trends in nitrate based on the combined Hebron and Lebanon data, and a significant change in specific conductance in a negative direction based on the Lebanon data (Fig. 20).

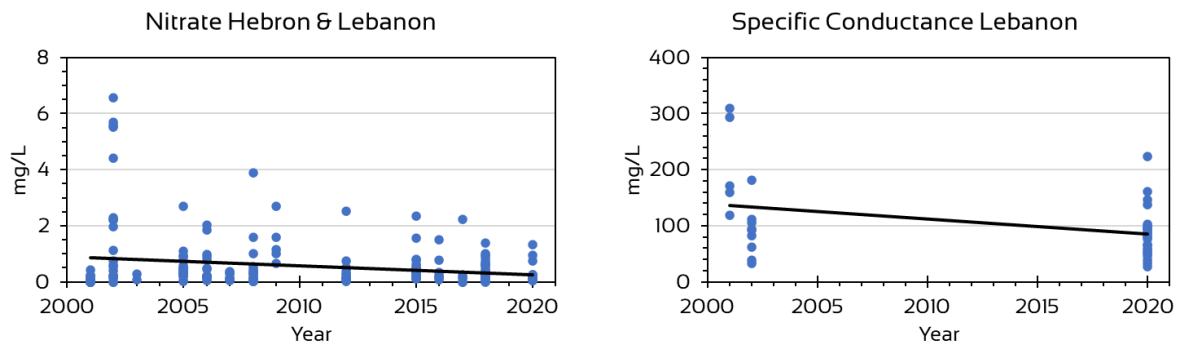


Figure 20. Linear regressions of nitrate over time from the combined Hebron and Lebanon dataset, and specific conductance over time from the Lebanon dataset.

It is somewhat paradoxical that nutrients and specific conductance are trending upward in Amston Lake, but trending downward in stormwater datasets. The stormwater specific conductance data is limited which may influence results. The stormwater nutrient dataset is more robust and thus more trustworthy.

The paradox suggested that increasing nutrients may be less related to distant sources in the watershed and more related to near-lake or autochthonous (derived within) sources. To further investigate, we broke out epilimnetic and hypolimnetic data from the ammonia, total phosphorus, and specific conductivity datasets (Fig. 21), albeit the changes in the subsets were not significant based on the ANOVA. Additionally, the lack of variance in the epilimnetic total phosphorus data precluded its statistical analysis.

It is not uncommon in aging lakes for ammonia concentrations in the hypolimnion to trend upwards over time. This is due to increased levels of anaerobic respiration in the hypolimnion which would rely first on oxidized forms of nitrogen (e.g., nitrate) with ammonia as a bi-product. The increasing ammonia levels in the epilimnion is not as easily explained. Ammonia is quickly used by plants and algae and not commonly detected in the epilimnion. One possible explanation is the influence of groundwater

contaminated with ammonia from improperly functioning onsite sewage treatment systems.

The trend in increasing hypolimnetic total phosphorus levels over time is more discernible than epilimnetic trend due to the nature of the dataset; it may be worth requesting that additional resolution be provided for phosphorus data from the lab. Phosphorus loading in the hypolimnion does occur at Amston Lake and occurred in 2020 (Fig. 3). However, it does not appear to have increased epilimnetic level or algal productivity at this time.

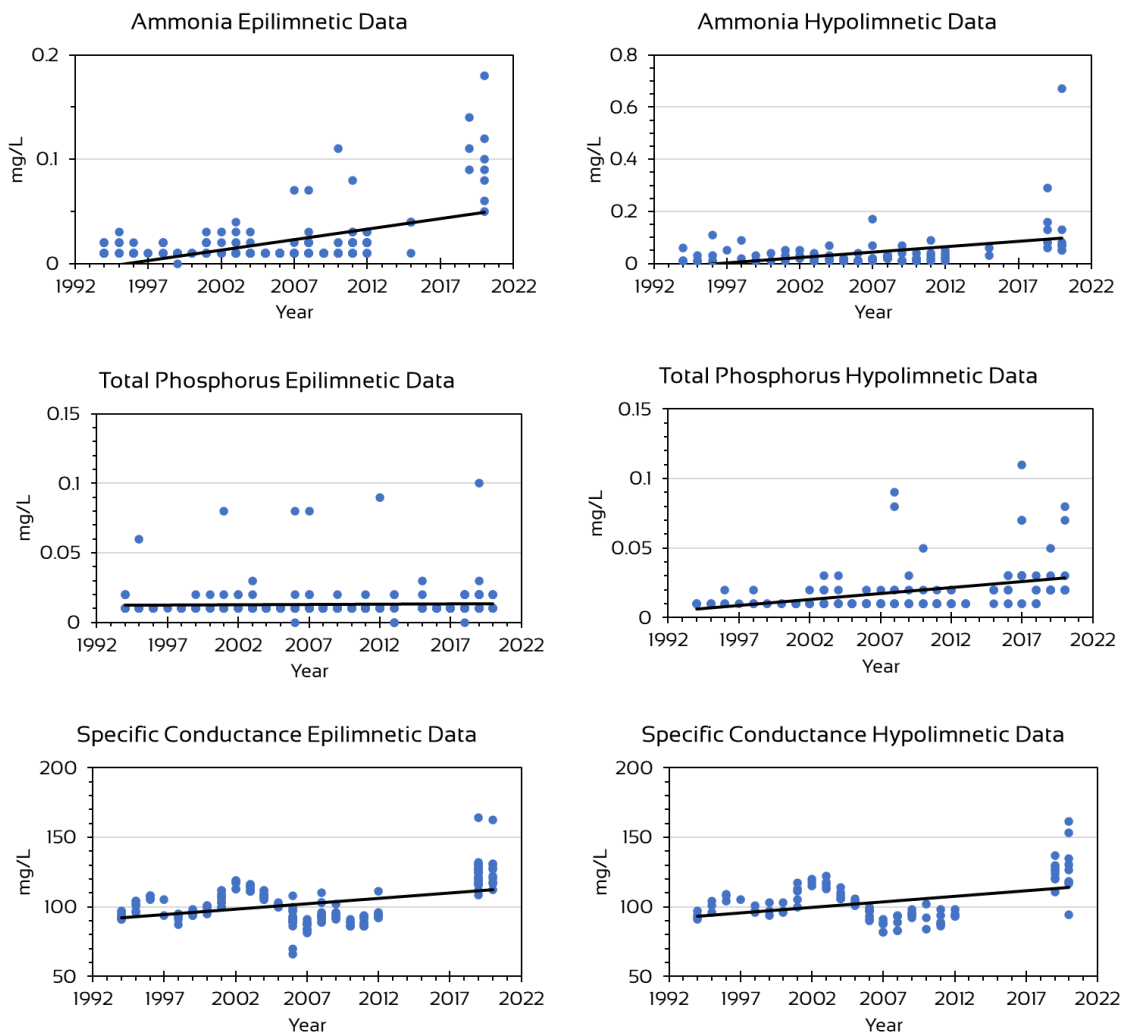


Figure 21. Regression analyses of epilimnetic and hypolimnetic ammonia, total phosphorus and specific conductance over time since 1994.

RECOMMENDATIONS

The lake water quality and stormwater monitoring programs of the ALTD Lake Health Committee effectively provide the data and water samples necessary to assess conditions and detect trends. On occasion we do see data that looks to be anomalous (e.g., the October 20th epilimnetic specific conductance). One method of assuring quality data is to have it analyzed by two independent parties. We recommend that a portion of the laboratory analyses performed by the Lake Health Committee (e.g., specific conductance, pH, total dissolved solids) also be performed by Phoenix Environmental Laboratories in 2021. Results from paired data can be statistically analyzed in the 2021 report.

The difference in nutrient concentrations in April 9th samples over the May 1st samples was notable. It will be important in the future to collect stormwater samples as early as in the season to catch the true first flush.

We have suggested that groundwater contaminated with ammonia from onsite sewage systems might be responsible for the historical increase in epilimnetic ammonia levels. Much of the shoreline and watershed is connected to a central sewer system. It may be useful to develop a study to determine if there is an influence from contaminated groundwater. Analytes such as boron are not expensive to test. AER could provide a study design and/or collect samples and report on results.

REFERENCES

- Aquatic Ecosystem Research (AER). 2019. Results – Statistical Analysis of Storm Water Data. Memo transmitted Amston Lake District on May 24, 2019.
- Bell, M. 1985. The Face of Connecticut. State Geological and Natural History Survey of Connecticut. Bull. 110.
- [CT DE] Connecticut Department of Environmental Protection (CT DEP). 1991. Trophic Classifications of Forty-nine Connecticut Lakes. CT DEEP, Hartford, CT. 98 pp.
- [CT DPH] Connecticut Department of Public Health. 2010. Presence of Total Coli-form or Fecal Coliform/ E. coli Bacteria in the Water Supply At Food Service Establishments. https://portal.ct.gov/-/media/Departments-and-Agen-cies/DPH/dph/drinking_water/pdf/PresenceofTotalColiformatFoodServicepdf.pdf?la=en
- [CT DPH] Connecticut Department of Public Health. 2016. State of Connecticut Guidelines for Monitoring Swimming Water and Closure Protocol. https://portal.ct.gov/-/media/Departments-and-Agencies/DPH/dph/environmental_health/BEACH/Guidelines-for-Monitoring-Swimming-Water-and-Closure-Protocol-March-2016.pdf
- [CT DPH & CT DEEP] Connecticut Department of Public Health and Connecticut Department of Energy and Environmental Protection. 2019. Guidance to Local Health Departments for Blue–Green Algae Blooms in Recreational Freshwaters. See https://portal.ct.gov/-/media/Departments-and-Agencies/DPH/dph/environmental_health/BEACH/Blue-Green-AlgaeBlooms_June2019_FINAL.pdf?la=en
- [ECRCDA] Eastern Connecticut Resource Conservation and Development – Environmental Review Team. 1985. *Amston Lake – Hebron, CT*. http://cert.org/pdfs/Hebron_AmstonLake_312.pdf
- Frink CR, Norvell WA. 1984. Chemical and physical properties of Connecticut lakes. New Haven (CT): Connecticut Agricultural Experiment Station. Bulletin 817. 180 pp
- Jacobs RP, O'Donnell EB. 2002. A fisheries guide to lakes and ponds of Connecticut, including the Connecticut River and its coves. Hartford (CT): Connecticut Department of Energy and Environmental Protection, Bulletin No. 35.
- Lawton L, Marsalek B, Padisák J., Chorus I. 1999. DETERMINATION OF CYANOBACTERIA IN THE LABORATORY. In Toxic Cyanobacteria in Water: A guide to their public health consequences, monitoring and management. Chorus and Bartram, eds.
- McMaster NL & DW Schindler. 2005. Planktonic and Epipelagic Algal Communities and their Relationship to Physical and Chemical Variables in Alpine Ponds in Banff National Park, Canada, Arctic, Antarctic, and Alpine Research, 37:3, 337-347, DOI: 10.1657/1523-0430(2005)037[0337:PAEACA]2.0.CO;2
- Redfield A.C. 1958. The biological control of chemical factors in the environment. American Scientist. 46(3):205-221.
- Siver, P.A. 1993. Inferring lakewater specific conductivity with scaled chrysophytes. Limnol. Oceanogr. 38: 1480-1492

Timoshkina, O.A., M.V.Moore, N.N.Kulikova, I.V.Tomberg, V.V.Malnik, M.N.Shimaraev, E.S.Troitskaya, A.A.Shirokaya, V.N.Sinyukovich, E.P.Zaitseva, V.M.Domysheva, M.Yamamuro, A.E.Poberezhnaya, E.M.Timoshkinaa. 2018. Groundwater contamination by sewage causes benthic algal outbreaks in the littoral zone of Lake Baikal (East Siberia). *J. Great Lakes Research*. 44 (2):230-244.

Wetzel RG. 2001. *Limnology Lake and River Ecology*. 3rd Ed. Academic Press. 1006 pp.

APPENDIX A. ALGAL COMMUNITY DATA

Cyano = Cyanobacteria; Chloro = Chlorophyta; Chryso = Chrysophyta; Bacillario = Bacillariophyta; Pyrro = Pyrrophyta; Crypto = Cryptophyta; and Eugleno = Euglenophyta

		7-May-20	2-Jun-20	2-Jul-20	29-Jul-20	26-Aug-20	24-Sep-20	20-Oct-20
CYANO	<i>Aphanizomenon sp.</i>	X						
	<i>Aphanocapsa sp.</i>			X	X	X	X	X
	<i>Aphanothece sp.</i>				X		X	X
	<i>Chroococcus sp.</i>					X		
	<i>Dolichospermum sp.</i>			X	X	X	X	X
	<i>Lyngbya sp.</i>							X
	<i>Microcystis sp.</i>			X	X	X	X	X
	<i>Oscillatoria sp.</i>	X	X	X				
	<i>Rhabdoderma sp.</i>	X						
	<i>Snowella sp.</i>					X	X	
	<i>Woronichinia sp.</i>		X		X	X	X	
CHLORO	<i>Anikistrodesmus sp.</i>		X			X	X	
	<i>Chlorella sp.</i>				X			
	<i>Closterium sp.</i>			X	X	X		
	<i>Coelastrum sp.</i>			X	X	X	X	X
	<i>Cosmarium sp.</i>				X			
	<i>Dictyosphaerium sp.</i>				X			
	<i>Elakatothrix sp.</i>		X	X	X	X	X	X
	<i>Eudorina sp.</i>					X	X	
	<i>Gloeocystis sp.</i>	X	X	X	X	X	X	X
	<i>Gonium sp.</i>			X	X			
	<i>Kirchneriella</i>	X		X	X			
	<i>Nephrocytium sp.</i>			X	X	X		X
	<i>Oocystis</i>		X	X	X	X	X	X
	<i>Padorina sp.</i>			X				
	<i>Quadrigula sp.</i>		X	X	X	X		X



	<i>Scenedesmus sp.</i>				X	X		
	<i>Selenastrum sp.</i>		X	X	X		X	X
	<i>Sphaerocystis sp.</i>					X	X	X
	<i>Staurastrum sp.</i>			X	X	X	X	
	<i>Tetraedron sp.</i>		X					
	<i>Xanthidium sp.</i>	X						
CHRYSO	<i>Chrysosphaera sp.</i>							X
	<i>Dinobryon sp.</i>	X		X	X			
	<i>Mallomonas sp.</i>		X	X	X	X	X	X
	<i>Synura sp.</i>		X				X	X
	<i>Uroglenopsis sp.</i>	X	X	X	X	X	X	
BACILLARIO	<i>Cyclotella sp.</i>		X				X	X
	<i>Fragilaria sp.</i>		X					
	<i>Synedra sp.</i>				X	X	X	
	<i>Tabellaria sp.</i>	X	X		X			
PYRRHO	<i>Ceratium sp.</i>		X	X	X	X	X	X
	<i>Peridinium sp.</i>	X						
CRYPTO	<i>Cryptomonas ovata</i>	X	X	X	X		X	X
EUGLENO	<i>Trachelomonas sp.</i>	X	X	X	X	X	X	X
	Total	12	18	22	28	24	23	20



May 7, 2020

Taxa	Genus / species	Cells / mL	%	Taxa cells / mL	Taxa %
Cyanophyta	<i>Aphanizomenon sp.</i>	0	0.0	36	2.6
	<i>Aphanocapsa sp.</i>	0	0.0		
	<i>Dolichospermum sp.</i>	0	0.0		
	<i>Microcystis sp.</i>	0	0.0		
	<i>Rhododerma sp.</i>	36	2.6		
	<i>Woronichinia sp.</i>	0	0.0		
Chlorophyta	<i>Anikistrodesmus sp.</i>	0	0.0	416	30.9
	<i>Kirchniriella sp.</i>	416	30.9		
	<i>Micractinium sp.</i>	0	0.0		
	<i>Mougiotia sp.</i>	0	0.0		
	<i>Tetraedron sp.</i>	0	0.0		
Chrysophyta	<i>Mallomonas sp.</i>	0	0.0	875	64.9
	<i>Uroglenopsis sp.</i>	875	64.9		
Bacillariophyta	<i>Asterionella formosa</i>	0	0.0	0	0.0
	<i>Aulocoseria sp.</i>	0	0.0		
Dinophyceae	<i>Ceratium sp.</i>	0	0.0	0	0.0
Cryptophyceae	<i>Cryptomonas ovata</i>	4	0.3	4	0.3
	<i>Rhodomonas sp.</i>	0	0.0		
Euglenophyceae	<i>Euglena sp.</i>	0	0.0	0	0.0
	<i>Phacus sp.</i>	0	0.0		
	<i>Trachelomonas sp.</i>	0	0.0		
	Unknown	18	1.3	18	1.3
Taxa identified					
4	Totals	1349	100	1349	100

June 2, 2020

Taxa	Genus / species	Cells / mL	%	Taxa cells / mL	Taxa %
Cyanophyta	<i>Aphanizomenon sp.</i>	0	0.0	173	32.6
	<i>Aphanocapsa sp.</i>	0	0.0		
	<i>Oscillatoria sp.</i>	173	32.6		
	<i>Woronichinia sp.</i>	0	0.0		
Chlorophyta	<i>Anikistrodesmus sp.</i>	0	0.0	190	35.9
	<i>Gloeocystis sp.</i>	181	34.1		
	<i>Gonium sp.</i>	0	0.0		
	<i>Selenastrum sp.</i>	8	1.5		
	<i>Tetraedron sp.</i>	2	0.3		
Chrysophyta	<i>Mallomonas sp.</i>	0	0.0	93	17.6
	<i>Synura sp.</i>	22	4.1		
	<i>Uroglenopsis sp.</i>	72	13.5		
Bacillariophyta	<i>Asterionella formosa</i>	0	0.0	19	3.5
	<i>Cyclotella sp.</i>	12	2.4		
	<i>Tabellaria sp.</i>	6	1.2		
	<i>Synedra sp.</i>	0	0.0		
Dinophyceae	<i>Ceratium sp.</i>	0	0.0	0	0.0
	<i>Peridinium sp.</i>	0	0.0		
Cryptophyceae	<i>Cryptomonas ovata</i>	39	7.4	39	7.4
Euglenophyceae	<i>Euglena sp.</i>	0	0.0	2	0.3
	<i>Trachelomonas sp.</i>	2	0.3		
	<i>Unknown</i>	14	2.6	14	2.6
Taxa identified					
10	<i>Totals</i>	530	100	530	100

July 2, 2020

Taxa	Genus / species	Cells / mL	%	Taxa cells / mL	Taxa %
Cyanophyta	<i>Aphanizomenon sp.</i>	0	0.0	401	12.2
	<i>Aphanocapsa sp.</i>	319	9.7		
	<i>Dolichospermum sp.</i>	76	2.3		
	<i>Microcystis sp.</i>	6	0.2		
	<i>Woronichinia sp.</i>	0	0.0		
Chlorophyta	<i>Anikistrodesmus sp.</i>	0	0.0	2440	73.9
	<i>Coelastrum sp.</i>	178	5.4		
	<i>Closterium sp.</i>	6	0.2		
	<i>Elakatothrix sp.</i>	191	5.8		
	<i>Gloeocystis sp.</i>	1962	59.5		
	<i>Kirchniriella sp.</i>	6	0.2		
	<i>Nephrocytium sp.</i>	6	0.2		
	<i>Oocystis sp.</i>	13	0.4		
	<i>Quadrigula sp.</i>	45	1.4		
	<i>Selenastrum sp.</i>	25	0.8		
	<i>Staurastrum sp.</i>	6	0.2		
Chrysophyta	<i>Mallomonas sp.</i>	6	0.2	408	12.4
	<i>Dinobryon sp.</i>	389	11.8		
	<i>Uroglenopsis sp.</i>	13	0.4		
Bacillariophyta	<i>Asterionella formosa</i>	0	0.0	0	0.0
	<i>Stephanodiscus sp.</i>	0	0.0		
	<i>Synedra sp.</i>	0	0.0		
	<i>Pennate Diatom</i>	0	0.0		
Dinophyceae	<i>Ceratium sp.</i>	13	0.4	13	0.4
	<i>Glenodinium sp.</i>	0	0.0		
Cryptophyceae	<i>Cryptomonas ovata</i>	19	0.6	19	0.6
Euglenophyceae	<i>Euglena sp.</i>	0	0.0	6	0.2
	<i>Phacus sp.</i>	0	0.0		
	<i>Trachelomonas sp.</i>	6	0.2		
	<i>Unknown</i>	13	0.4	13	0.4
Taxa identified					
19	<i>Totals</i>	3300	100	3300	100

July 29, 2020

Taxa	Genus / species	Cells / mL	%	Taxa cells / mL	Taxa %
Cyanophyta	<i>Aphanizomenon sp.</i>	0	0.0	3462	55.5
	<i>Aphanocapsa sp.</i>	1094	17.5		
	<i>Aphanothece sp.</i>	772	12.4		
	<i>Microcystis sp.</i>	624	10.0		
	<i>Oscillatoria sp.</i>	0	0.0		
	<i>Woronichinia sp.</i>	972	15.6		
Chlorophyta	<i>Anikistrodesmus sp.</i>	0	0.0	2716	43.6
	<i>Coelastrum sp.</i>	1030	16.5		
	<i>Chlorella sp.</i>	6	0.1		
	<i>Gloeocystis sp.</i>	1442	23.1		
	<i>Gonium sp.</i>	6	0.1		
	<i>Nephrocytium sp.</i>	154	2.5		
	<i>Oocystis sp.</i>	26	0.4		
	<i>Scenedesumus sp.</i>	26	0.4		
	<i>Selenastrum sp.</i>	19	0.3		
	<i>Staurastrum sp.</i>	6	0.1		
Chrysophyta	<i>Mallomonas sp.</i>	6	0.1	6	0.1
	<i>Uroglenopsis sp.</i>	0	0.0		
Bacillariophyta	<i>Asterionella formosa</i>	0	0.0	6	0.1
	<i>Tabellaria sp.</i>	6	0.1		
Dinophyceae	<i>Ceratium sp.</i>	6	0.1	6	0.1
	<i>Peridinium sp.</i>	0	0.0		
	<i>Gymnodinium sp.</i>	0	0.0		
	<i>Glenodinium sp.</i>	0	0.0		
Cryptophyceae	<i>Cryptomonas ovata</i>	13	0.2	13	0.2
Euglenophyceae	<i>Euglena sp.</i>	0	0.0	6	0.1
	<i>Trachelomonas sp.</i>	6	0.1		
	<i>Unknown</i>	19	0.3		
Taxa identified					
18	Totals	6236	100	6236	100

August 26, 2020

Taxa	Genus / species	Cells / mL	%	Taxa cells / mL	Taxa %
Cyanophyta	<i>Aphanizomenon sp.</i>	0	0.0	2183	67.6
	<i>Aphanocapsa sp.</i>	772	23.9		
	<i>Chroococcus sp.</i>	5	0.1		
	<i>Dolichospermum sp.</i>	127	3.9		
	<i>Microcystis sp.</i>	1271	39.3		
	<i>Rhododerman sp.</i>	5	0.1		
	<i>Woronichinia sp.</i>	5	0.1		
Chlorophyta	<i>Anikistrodesmus sp.</i>	18	0.6	989	30.6
	<i>Elakatothrix sp.</i>	9	0.3		
	<i>Eudorina elegans</i>	73	2.2		
	<i>Gloeocystis sp.</i>	744	23.0		
	<i>Nephrocytium sp.</i>	18	0.6		
	<i>Oocystis sp.</i>	14	0.4		
	<i>Quadrigula sp.</i>	36	1.1		
	<i>Scenedesumus sp</i>	18	0.6		
	<i>Sphaerocystis sp.</i>	54	1.7		
	<i>Staurastrum sp.</i>	5	0.1		
Chrysophyta	<i>Mallomonas sp.</i>	0	0.0	9	0.3
	<i>Uroglenopsis sp.</i>	9	0.3		
Bacillariophyta	<i>Asterionella formosa</i>	0	0.0	18	0.6
	<i>Synedra sp.</i>	18	0.6		
Dinophyceae	<i>Ceratium sp.</i>	5	0.1	5	0.1
	<i>Glenodinium sp.</i>	0	0.0		
Cryptophyceae	<i>Cryptomonas ovata</i>	0	0.0	0	0.0
	<i>Rhodomonas sp.</i>	0	0.0		
Euglenophyceae	<i>Euglena sp.</i>	0	0.0	5	0.1
	<i>Trachelomonas sp.</i>	5	0.1		
	<i>Unknown</i>	23	0.7		
Taxa identified					
20	Totals	3232	100	3232	100

September 24, 2020

Taxa	Genus / species	Cells / mL	%	Taxa cells / mL	Taxa %
Cyanophyta	<i>Aphanizomenon sp.</i>	0	0.0	1248	79.8
	<i>Aphanocapsa sp.</i>	3	0.2		
	<i>Dolichospermum sp.</i>	10	0.7		
	<i>Microcystis sp.</i>	418	26.8		
	<i>Snowella sp.</i>	329	21.1		
	<i>Woronichinia sp.</i>	487	31.1		
Chlorophyta	<i>Anikistrodesmus sp.</i>	7	0.4	202	12.9
	<i>Gloeocystis sp.</i>	165	10.5		
	<i>Oocystis sp.</i>	17	1.1		
	<i>Pediastrum sp.</i>	0	0.0		
	<i>Selenastrum sp.</i>	7	0.4		
	<i>Staurastrum sp.</i>	7	0.4		
Chrysophyta	<i>Mallomonas sp.</i>	14	0.9	51	3.3
	<i>Dinobryon sp.</i>	0	0.0		
	<i>Synura sp.</i>	7	0.4		
	<i>Uroglenopsis sp.</i>	31	2.0		
Bacillariophyta	<i>Asterionella formosa</i>	0	0.0	14	0.9
	<i>Aulocoseria sp.</i>	0	0.0		
	<i>Cyclotella sp.</i>	7	0.4		
	<i>Synedra sp.</i>	7	0.4		
	<i>Pennate Diatom</i>	0	0.0		
Dinophyceae	<i>Ceratium sp.</i>	3	0.2	3	0.2
	<i>Glenodinium sp.</i>	0	0.0		
Cryptophyceae	<i>Cryptomonas ovata</i>	41	2.6	41	2.6
	<i>Rhodomonas sp.</i>	0	0.0		
Euglenophyceae	<i>Euglena sp.</i>	0	0.0	3	0.2
	<i>Trachelomonas sp.</i>	3	0.2		
	<i>Unknown</i>	0	0.0		
Taxa identified					
18	Totals	1564	100	1564	100

October 20, 2020

Taxa	Genus / species	Cells / mL	%	Taxa cells / mL	Taxa %
Cyanophyta	<i>Aphanizomenon sp.</i>	0	0.0	4098	98.0
	<i>Aphanocapsa sp.</i>	3026	72.4		
	<i>Dolichospermum sp.</i>	5	0.1		
	<i>Microcystis sp.</i>	1067	25.5		
	<i>Woronichinia sp.</i>	0	0.0		
Chlorophyta	<i>Anikistrodesmus sp.</i>	0	0.0	52	1.2
	<i>Gloeocystis sp.</i>	12	0.3		
	<i>Oocystis sp.</i>	29	0.7		
	<i>Selenastrum sp.</i>	5	0.1		
	<i>Sphaerocystis sp.</i>	6	0.1		
Chrysophyta	<i>Mallomonas sp.</i>	5	0.1	5	0.1
	<i>Uroglenopsis sp.</i>	0	0.0		
Bacillariophyta	<i>Asterionella formosa</i>	0	0.0	0	0.0
	<i>Aulocoseria sp.</i>	0	0.0		
Dinophyceae	<i>Ceratium sp.</i>	0	0.0	0	0.0
	<i>Glenodinium sp.</i>	0	0.0		
Cryptophyceae	<i>Cryptomonas ovata</i>	18	0.4	18	0.4
	<i>Rhodomonas sp.</i>	0	0.0		
Euglenophyceae	<i>Euglena sp.</i>	0	0.0	2	0.0
	<i>Trachelomonas sp.</i>	2	0.0		
	<i>Unknown</i>	8	0.2		
Taxa identified					
10	Totals	4182	100	4182	100

APPENDIX B. BASE CATIONS, CHLORIDE, AND ALKALINITY

Ca^{2+} = calcium; Mg^{2+} = magnesium, K^{+} = potassium; Na^{+} = sodium; Cl^{-} = chloride; and Alk = alkalinity



Date	Unit	Ca ²⁺	Mg ²⁺	K ⁺	Na ⁺	Cl ⁻	Alk
2-Jun	mg/L	7.11	1.49	1.8	13.1	21.5	14
	meq/L	0.36	0.12	0.05	0.57	0.62	0.28
2-Jul	mg/L	7.32	1.54	1.8	13.2	20.1	14.5
	meq/L	0.37	0.13	0.05	0.57	0.58	0.29
29-Jul	mg/L	7.26	1.52	1.80	13.40	23.20	16.30
	meq/L	0.36	0.13	0.05	0.58	0.67	0.33
26-Aug	mg/L	7.11	1.5	1.8	13.3	22.1	17.7
	meq/L	0.36	0.12	0.05	0.58	0.64	0.35
24-Sep	mg/L	7.43	1.67	1.8	14.1	23.9	17.6
	meq/L	0.37	0.14	0.05	0.61	0.69	0.35
20-Oct	mg/L	6.93	1.57	1.8	13.9	22.6	16
	meq/L	0.35	0.13	0.05	0.60	0.66	0.32
Average	mg/L	7.19	1.55	1.80	13.50	22.23	16.02
St. Dev.	mg/L	0.18	0.07	0.00	0.40	1.34	1.54
Average	meq/L	0.36	0.13	0.05	0.59	0.64	0.32
St. Dev.	meq/L	0.01	0.01	0.00	0.02	0.04	0.03



APPENDIX C. STATISTICAL ANALYSES

Alk	Alkalinity
NH3	Ammonia
TKN	Total Kjeldahl Nitrogen
TP	Total Phosphorus
pH	pH
Cond	Specific Conductance
Turb	Turbidity

MLR Whole

	Estimate	Std. Error	t value	Pr(> t)	
(Intercept)	2.03E+03	2.83E+00	714.3	< 2e-16	***
Alk	-1.19E-01	2.28E-02	-5.241	0.000534	***
NH3	1.07E+00	6.93E-01	1.546	0.156602	
TKN	-1.20E-01	6.59E-01	-0.182	0.85969	
TP	2.06E+01	6.70E+00	3.077	0.013202	*
pH	-7.61E-01	4.04E-01	-1.883	0.092353	.
Cond	1.55E-02	6.72E-03	2.3	0.047038	*

R 7.13E-01
p **5.00E-03**

MLR EPI Had to remove TP due to lack of variance

	Estimate	Std. Error	t value	Pr(> t)	
(Intercept)	2.02E+03	3.15E+00	640.53	3.56E-11	***
Alk	-2.16E-01	4.99E-02	-4.331	0.0123	*
NH3	4.68E+00	3.39E+00	-1.381	0.2395	
TKN	2.09E+00	2.20E+00	0.952	0.3951	
pH	6.15E-01	4.55E-01	1.351	0.248	
Cond	2.70E-03	6.93E-03	0.39	0.7165	

r 7.10E-01
p 6.36E-02

ANOVA Whole

	Df	Sum Sq	Mean Sq	F value	Pr(>F)	
Alk	1	0.32701	0.32701	4.9723	0.05271	.
NH3	1	0.55659	0.55659	8.463	0.01734	*
TKN	1	0.87892	0.87892	13.364	0.00527	**
TP	1	0.59643	0.59643	9.0688	0.01468	*
pH	1	0.13888	0.13888	2.1117	0.18013	
Cond	1	0.34776	0.34776	5.2877	0.04704	*

ANOVA

	Df	Sum Sq	Mean Sq	F value	Pr(>F)	
Alk	1	1.56842	1.56842	23.159	0.00857	**
NH3	1	0.04935	0.04935	0.7287	0.44141	
TKN	1	0.08512	0.08512	1.2569	0.32499	
pH	1	0.11591	0.11591	1.7116	0.26089	
Cond	1	0.0103	0.0103	0.1521	0.71645	
Residuals	4	0.27089	0.06772			



MLR HYP

	Estimate	Std. Error	t value	Pr(> t)
(Intercept)	2018.42	14.2995	141.15	5.02e-05 ***
Alk	-0.07638	0.06732	-1.135	0.374
NH3	-1.07239	1.18228	-0.907	0.46
TKN	-3.45266	3.79506	-0.91	0.459
TP	28.4026	20.4736	1.387	0.3
pH	-1.24579	2.38352	-0.523	0.653
Cond	0.10124	0.04139	2.446	0.134

R 0.75

p 0.1729

ANOVA

	Df	Sum Sq	Mean Sq	F value	Pr(>F)
Alk	1	0.07799	0.07799	1.2721	0.37649
NH3	1	0.32587	0.32587	5.3149	0.1476
TKN	1	0.90044	0.90044	14.686	0.06184
TP	1	0.14331	0.14331	2.3373	0.26591
pH	1	0.06293	0.06293	1.0263	0.41765
Cond	1	0.36683	0.36683	5.983	0.13428



**All Sites
MLR**

	Estimate	Std. Error	t value	Pr(> t)
(Intercept)	2014.98	2.75153	732.31	<2e-16
Nitrate	-1.1417	0.77239	-1.478	0.1452
TP	-13.391	5.4929	-2.438	0.0181
Cond	-0.022	0.01965	-1.118	0.2683
TURB	0.0297	0.02104	1.412	0.1637
R	0.1329			
p	0.01918			

**Hebron Only
MLR**

	Estimate	Std. Error	t value	Pr(> t)
(Intercept)	2005.16	4.36107	459.79	<2e-16
Nitrate	-0.5011	0.80393	-0.623	0.5385
TP	-14.402	6.56991	-2.192	0.0375
Cond	0.06612	0.03237	2.043	0.0513
TURB	0.07872	0.04002	1.967	0.0599
R	0.2174			
p	0.03332			

ANOVA

	Df	Sum Sq	Mean Sq	F value	Pr(>F)
Nitrate	1	420.9	420.88	5.7446	0.02 *
TP	1	229.3	229.34	3.1302	0.0825 .
Cond	1	139.4	139.43	1.9031	0.1734
TURB	1	146.1	146.08	1.9938	0.1637

ANOVA

	Df	Sum Sq	Mean Sq	F value	Pr(>F)
Nitrate	1	231.19	231.19	3.6443	0.0674
TP	1	181.49	181.49	2.8609	0.1027
Cond	1	113.19	113.19	1.7843	0.1932
TURB	1	245.48	245.48	3.8696	0.0599



**Lebanon Only
MLR**

	Estimate	Std. Error	t value	Pr(> t)
(Intercept)	2023.57	3.5047	577.39	< 2e-16
Nitrate	-5.8661	2.23508	-2.625	0.0152
TP	-20.397	11.2097	-1.82	0.0819
Cond	-0.0733	0.02247	-3.262	0.0034
TURB	0.04091	0.03123	1.31	0.2032
r	0.3432			
p	0.00763			

ANOVA

	Df	Sum Sq	Mean Sq	F value	Pr(>F)
Nitrate	1	216.5	216.5	3.7653	0.0647 .
TP	1	46.29	46.29	0.805	0.3789
Cond	1	678.24	678.24	11.796	0.0023 **
TURB	1	98.65	98.65	1.7157	0.2032

